Galactic/Extragalactic Cosmic Rays

Gaisser, *Front.Phys.(Beijing)* 8 (2013) 748-758

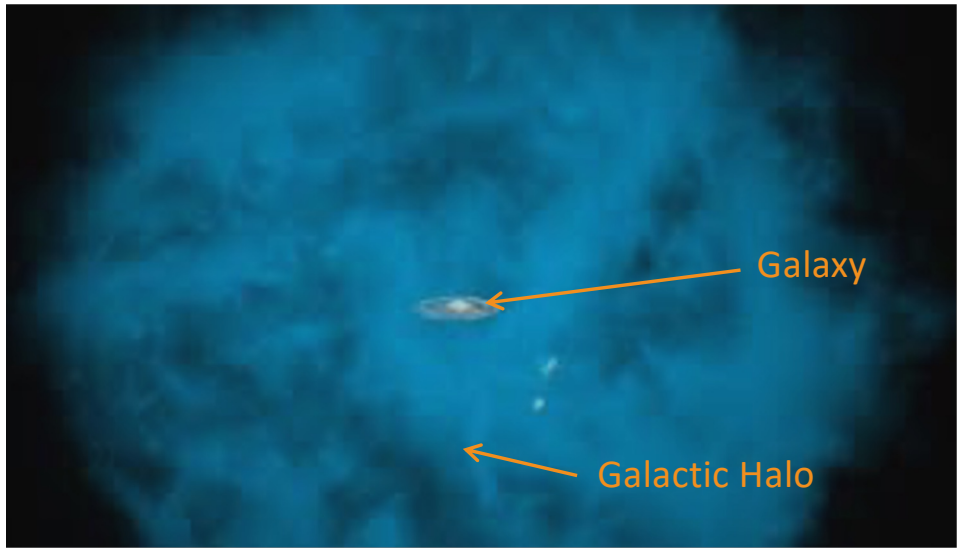

Galactic /Extragalactic CR Spectrum

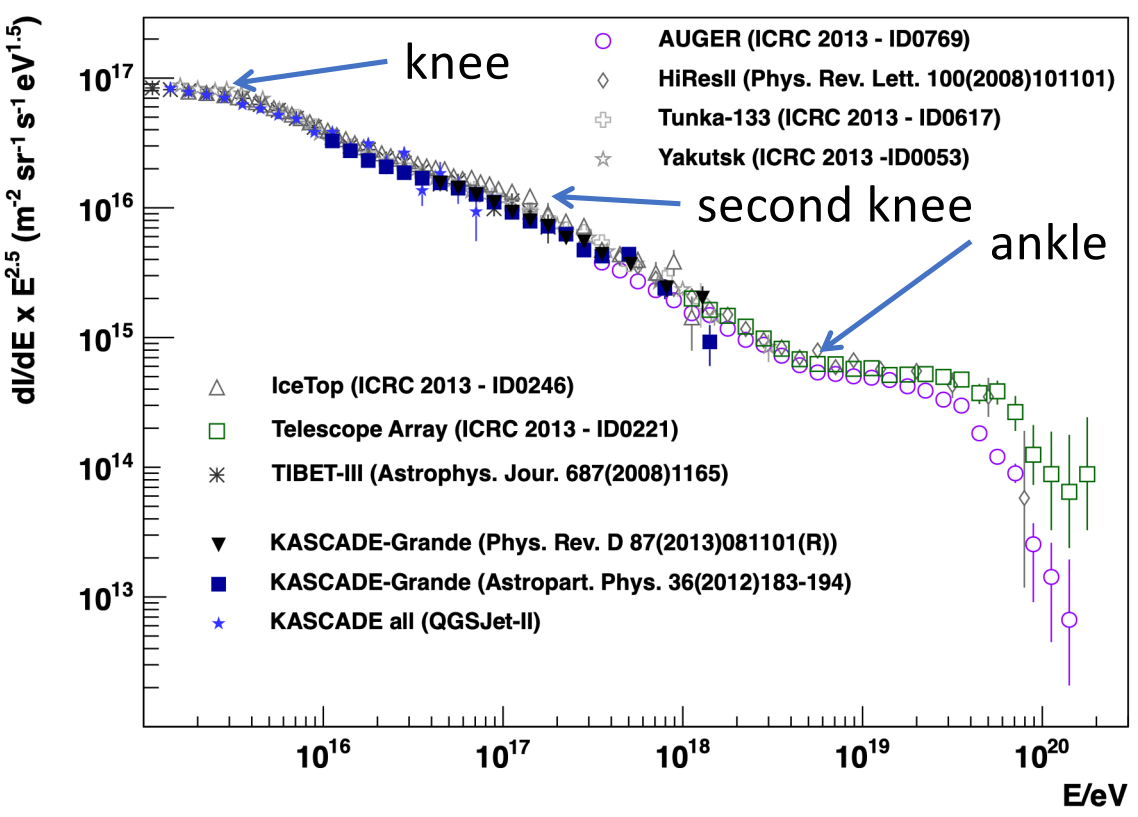

DESY.

Origins of the CR

The SNR Paradigm

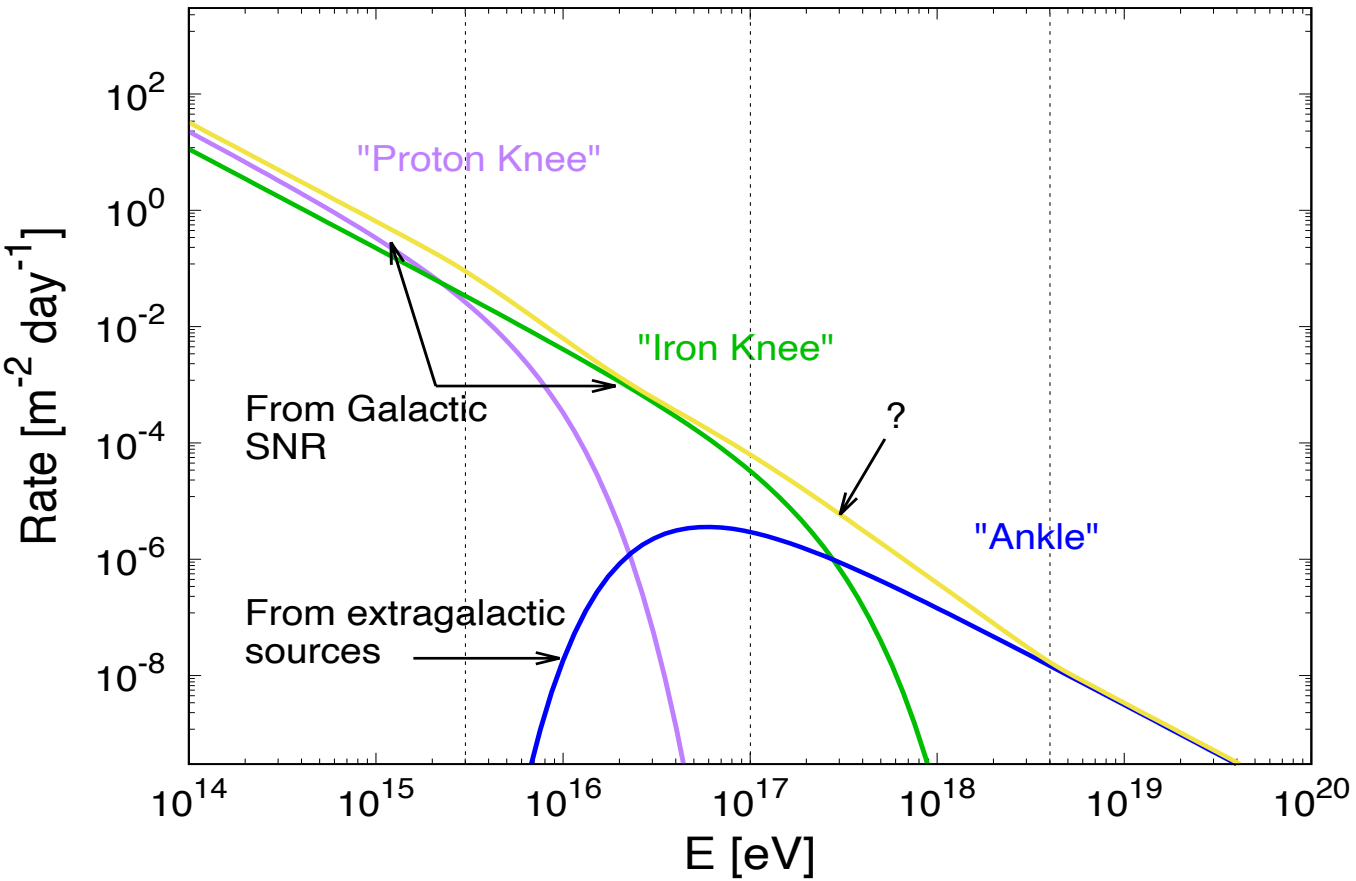

Galactic SNR, well motivated as a Galactic CR sources, are the preferred option for powering the spectrum all the way up to the knee proton energy ($10^{15.5}$ eV)

However, even if SNR accelerate CRs up to the proton knee, **a new source class is needed to fill the energy gap between 10^{17} eV and 10^{18} eV**

Taylor et al., Nature **volume 531**, pages 43–44 (2016)

The Need for a Population B

Original Plot (2005)

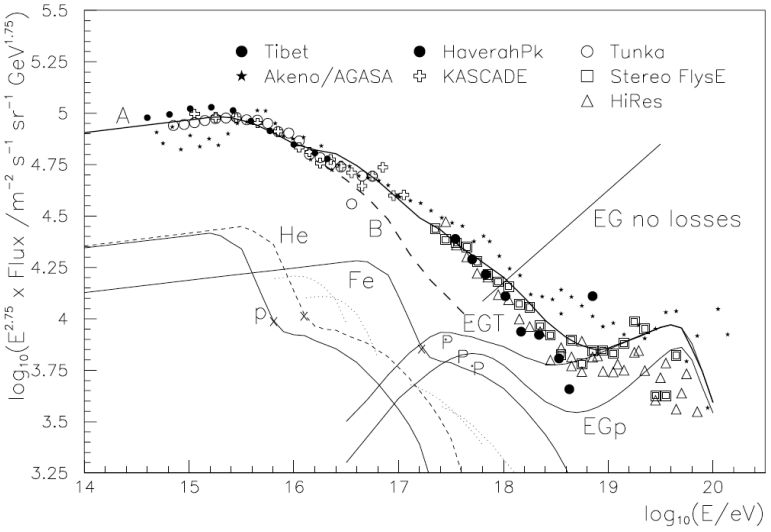

Hillas, 2005 *Nucl. Part. Phys.* **31** R95. (2005)

Revised Plot (2014)

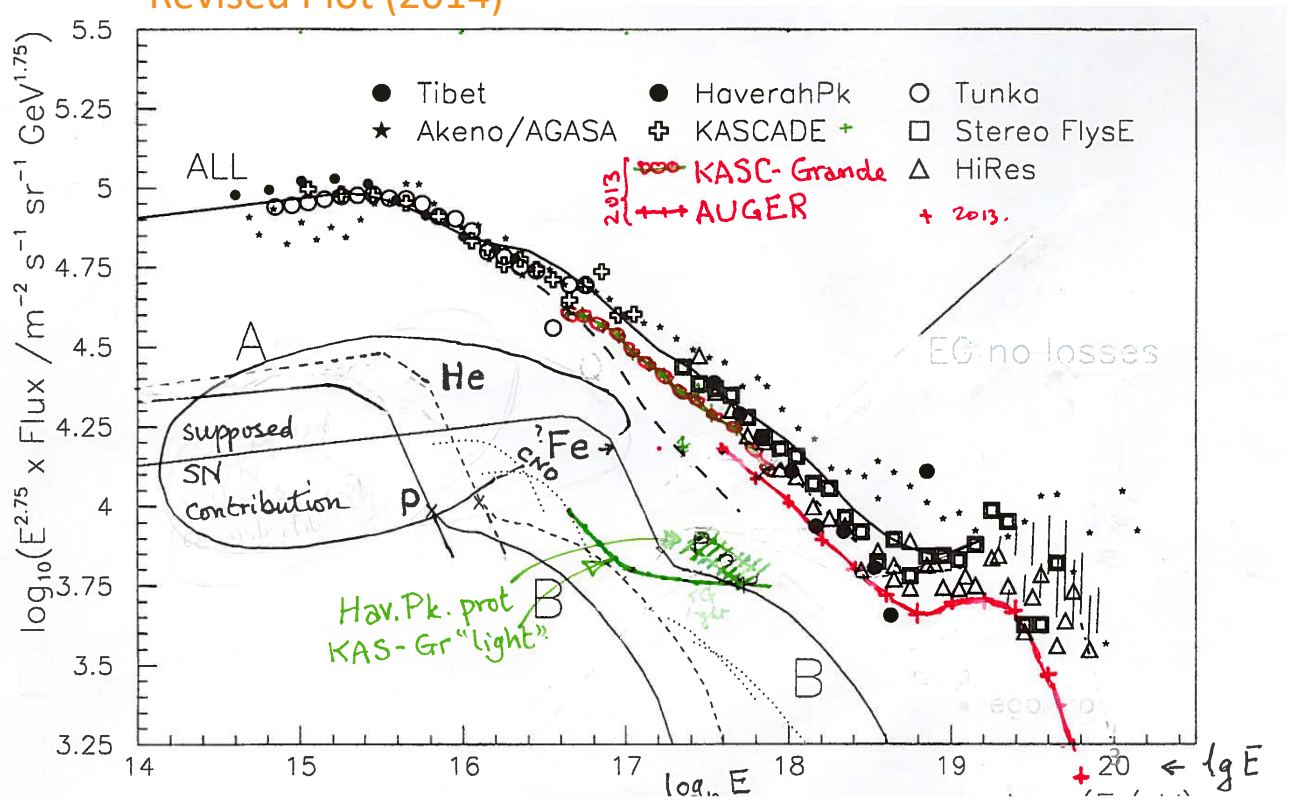

Pop A → Pop 1
Pop B → Pop 2
Pop C → Pop 3

Hillas-Type 3 Population Fit to the Transition Region

$$\frac{\mathbf{dN_{inj}}}{\mathbf{d\log E}} = \sum_{\mathbf{i}} \mathbf{a_i E^{-\gamma_i} e^{-(E/Z_i R_c)}}$$

Realisation of Hillas 3 Populations Scenario

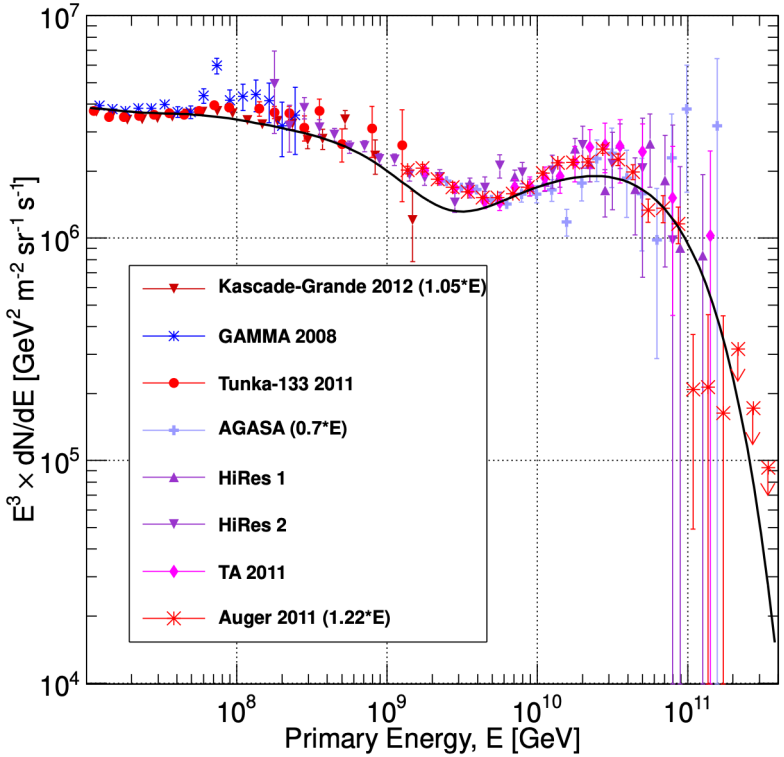

Galactic

Extragalactic?

	p	He	CNO	Mg-Si	Fe
Pop. 1:	7860	3550	2200	1430	2120
$R_c = 4$ PV	1.66	1.58	1.63	1.67	1.63
Pop. 2:	20	20	13.4	13.4	13.4
$R_c = 30$ PV	1.4	1.4	1.4	1.4	1.4
Pop. 3:	1.7	1.7	1.14	1.14	1.14
$R_c = 2$ EV	1.4	1.4	1.4	1.4	1.4

DESY.

Gaisser, Front. Phys., 2013, 8(6): 748–758 (2013)

Pop A → Pop 1
Pop B → Pop 2
Pop C → Pop 3

Gaisser-Type 3 Population Fit to the Transition Region

Alternative 3 Population Scenario

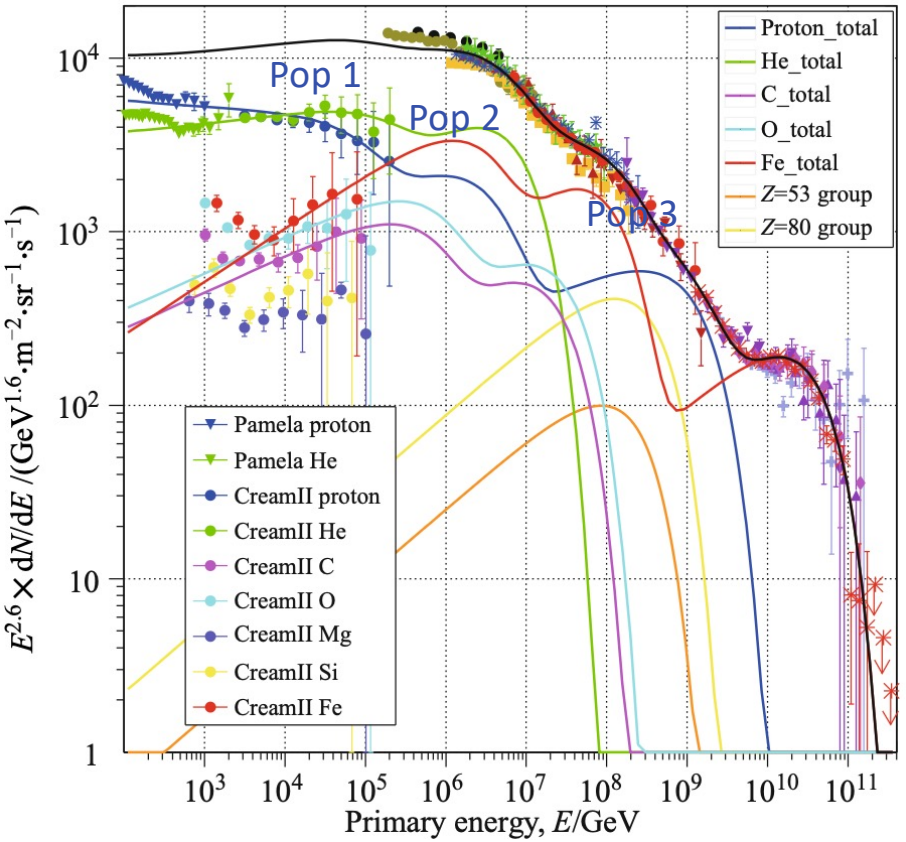

$$\frac{dN_{inj}}{d\log E} = \sum_i a_i E^{-\gamma_i} e^{-(E/Z_i R_c)}$$

Note: Pop A and Pop B max energy lowered by ~10-30 relative to Hillas' proposed scenario

	p	He	C	O	Fe	$50 < Z < 56$	$78 < Z < 82$
Pop. 1:	7000	3200	100	130	60		
$R_c = 120$ TV	1.66 1	1.58	1.4	1.4	1.3		
Pop. 2:	150	65	6	7	2.3	0.1	0.4
$R_c = 4$ PV	1.4	1.3	1.3	1.3	1.2	1.2	1.2
Pop. 3:	14				0.025		
$R_c = 1.3$ EV	1.4				1.2		
Pop. 2*:	150	65	6	7	2.1	0.1	0.53
$R_c = 4$ PV	1.4	1.3	1.3	1.3	1.2	1.2	1.2
Pop. 3*:	12				0.011		
$R_c = 1.5$ EV	1.4				1.2		

Gaisser, Front. Phys., 2013, 8(6): 748–758 (2013)

Note the Pop 2 proton component needs revising in light of recent LHAASO results: LHAASO Collaboration: 2511.05013

Constraints on at What Energy the Onset of Population B can Occur

CR Composition Evolution

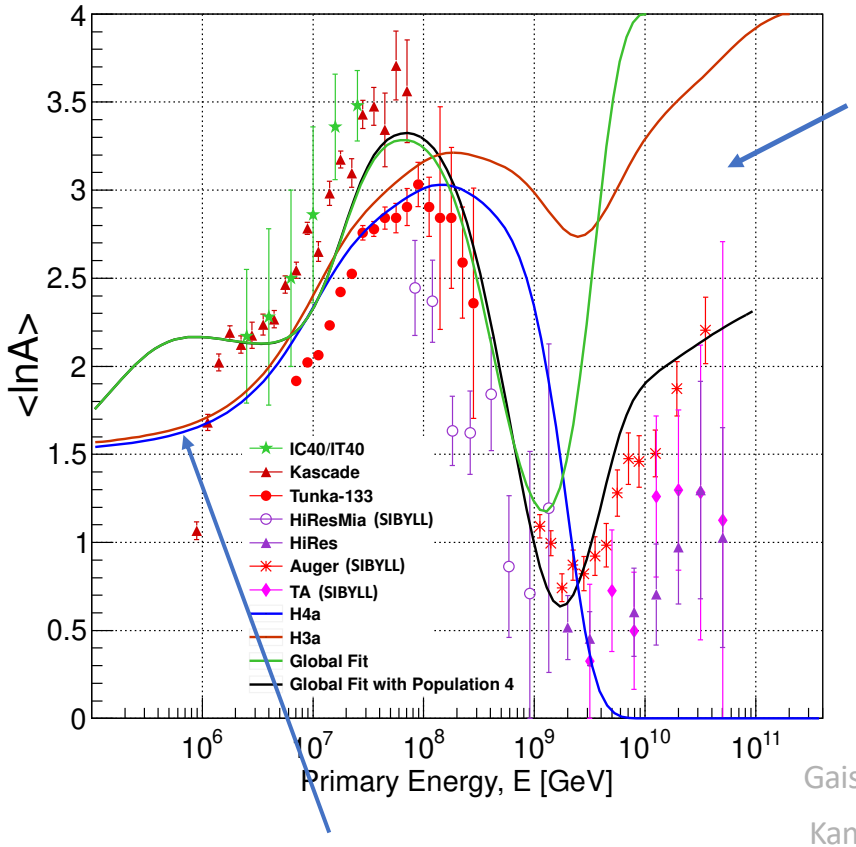

Only two clear light-heavy-light-heavy “cycles” in composition observed in data between the knee and the highest energies.

This places a strong constraint on the spacing of the energy onset in dominance of the new spectral components

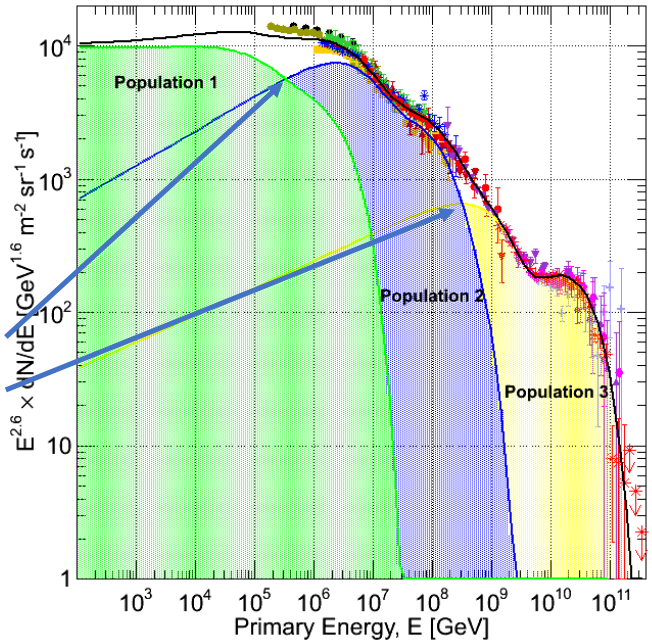

Gaisser, Front. Phys., 2013, 8(6): 748–758 (2013)

Kampert et al. **Astropart. Phys.** 35 10 660-678 (2012)

To be updated with LHAASO Coll., PRL 132, 131002 (2024)

Hillas & Gaisser-Type Population B Candidates:

Proton Spectrum

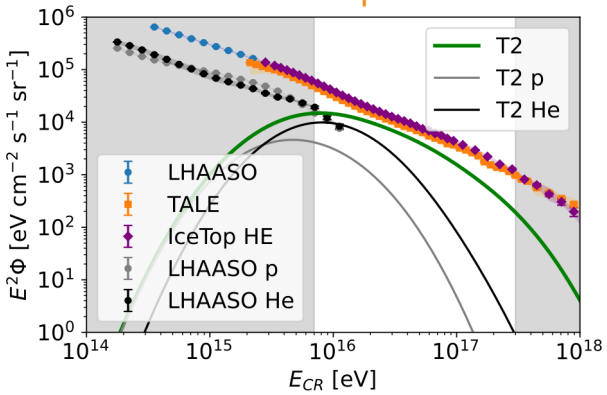

Composition

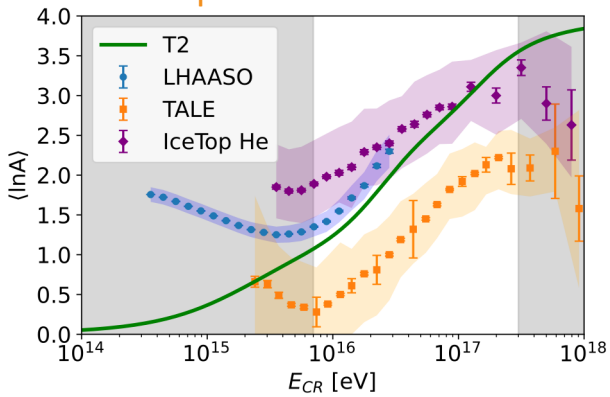

Extreme Supernovae (Type IIn): Hillas-Type Pop B

Ekanger et al., 2602.06410

Christofari et al., Astropart. Phys. 123 102492 (2020)

Zirakashvilli et al., Astropart. Phys. 78 28–34 (2016)

Supernovae in Massive Star Clusters: Gaisser-Type Pop B

Vieu et al., MNRAS 519, 136–147 (2023)

Proton Spectrum

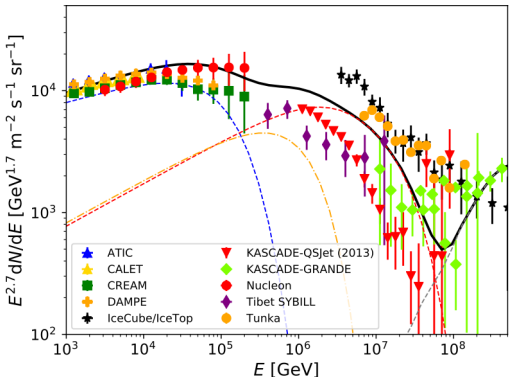

Composition

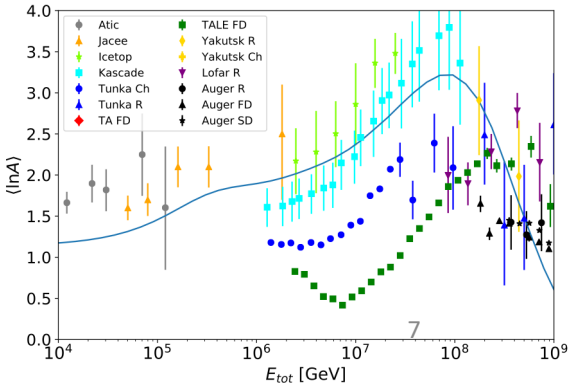

The Power Needs of Gaisser-Type Population B

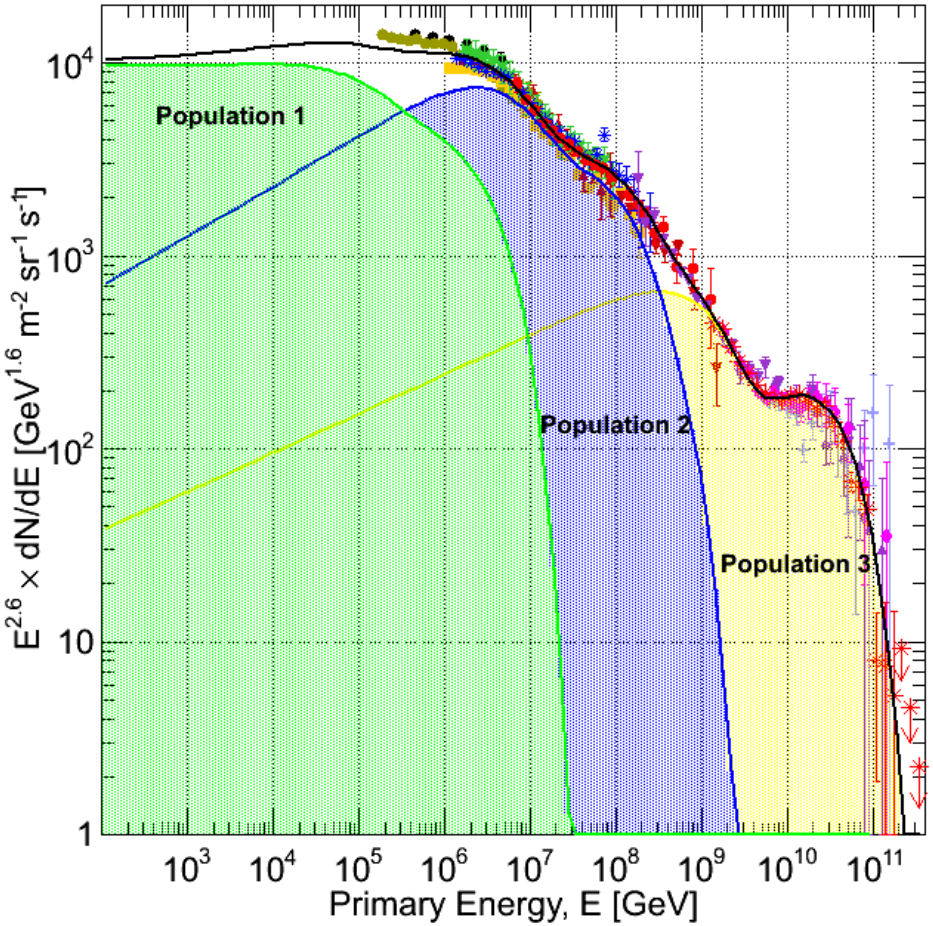

Gaisser, Front. Phys., 2013, 8(6): 748–758 (2013)

$$\mathbf{N_{ss} = Q_{CR}\tau_{esc.}}$$

$$\mathbf{\tau_{esc} = \tau_0 (E/E_0)^{-\delta}}$$

$$\mathbf{\delta = 0.33}$$

$$\mathbf{L_A \approx 10^{41}\ erg\ s^{-1}}$$

$$\mathbf{L_B \approx 2 \times 10^{39}\ erg\ s^{-1}}$$

Particle Accelerator Limits

$$t_{acc} = \eta \frac{R_{lar}}{c\beta^2}$$

$$t_{esc.} = \frac{R}{c\beta}$$

[AM Hillas (1984)]

$$E_{max} = \beta e B R$$

$$L_B = U_B 4\pi R^2 \beta c = \eta_B L_{KE}$$

[Lovelace et al. (1976)]

$$E_{max} < 2\,\mathrm{PeV} \left(\frac{L}{10^{38}\ \mathrm{erg\ s^{-1}}} \right)^{1/2} \left(\frac{\beta}{0.1} \frac{\eta_B}{0.1} \right)^{1/2}$$

Gaisser-Type Population B Candidates: Microquasars

$$\mathbf{E_{max} < 2PeV \left(\frac{L}{10^{38}\ erg\ s^{-1}} \right)^{1/2} \left(\frac{\beta}{0.1} \frac{\eta_B}{0.1} \right)^{1/2}}$$

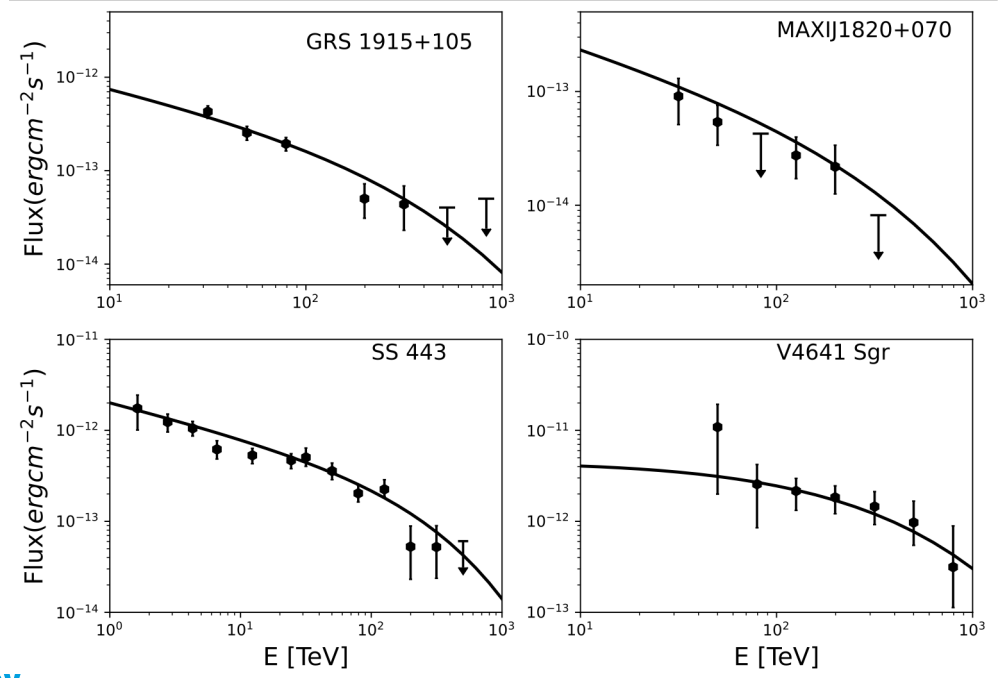

Nie et al., 2602.07620

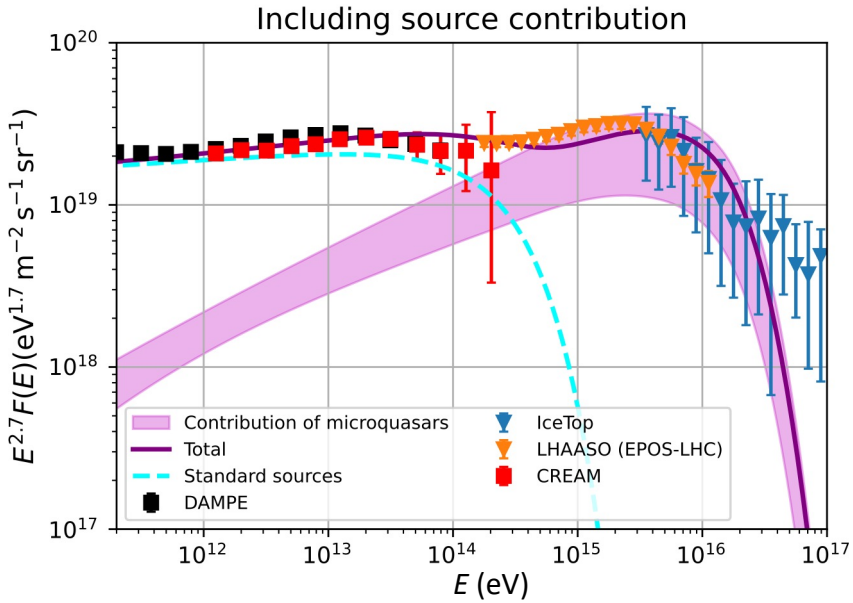

Kaci et al., 2510.01369

Aharonian et al., 2602.08223

Star Cluster Winds

Morlino et al., MNRAS 504, 6096–6105 (2021)

LHAASO Coll., Science Bulletin 69 (2024) 449–457

Population C Onset: Evidence for a Light Hard Spectrum

Kascade-Grande

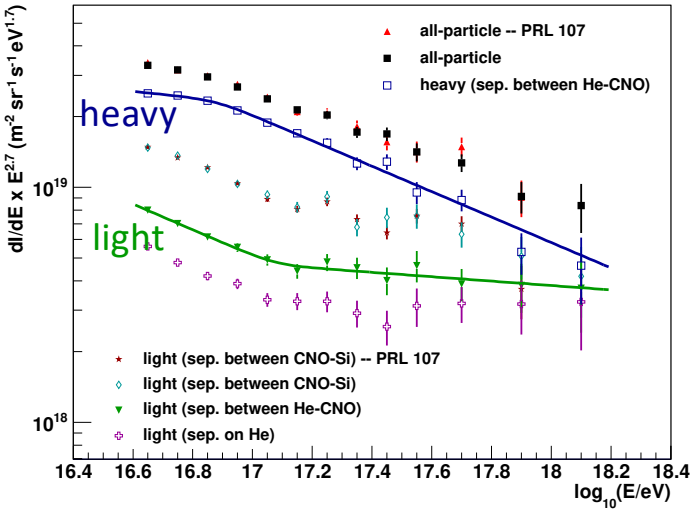

Apel et al., Phys. Rev. D 87, 081101 (2013)

A subdominant component of light CRs is seen $\gtrsim 10^{17}$ eV ("light ankle")

A recent reanalysis of the Kaskade-Grande data with updated hadronic models finds the same feature (though at somewhat lower energies)

Kang et al., *PoS* ICRC2025 (2025) 297

LHAASO-IceTop

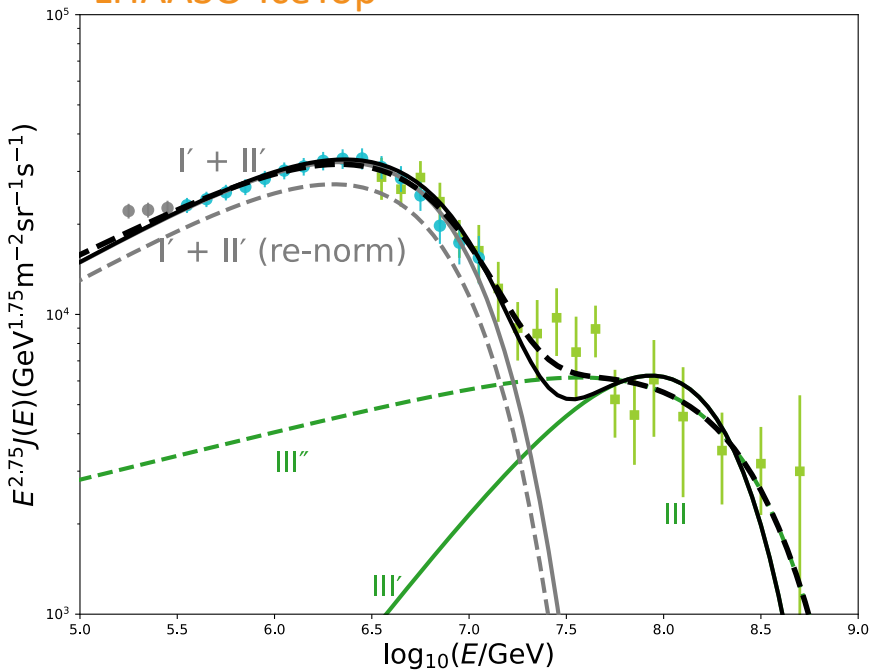

Aharonian et al., 2602.08223

The Source Evolution Scenario for the >$10^{17.7}$eV CRs

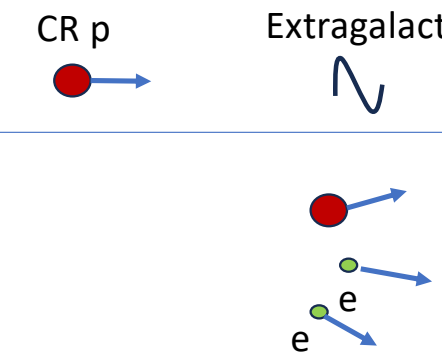

SFR evolution scenario

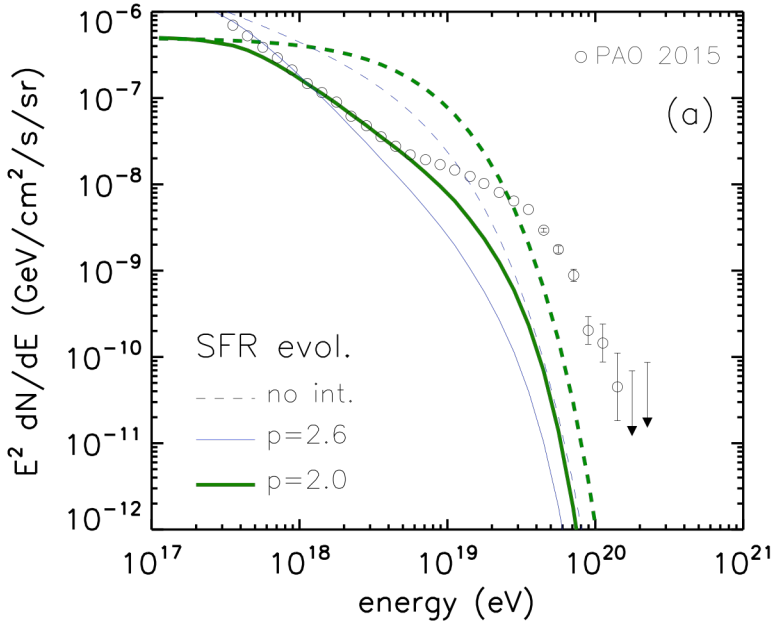

no evolution scenario

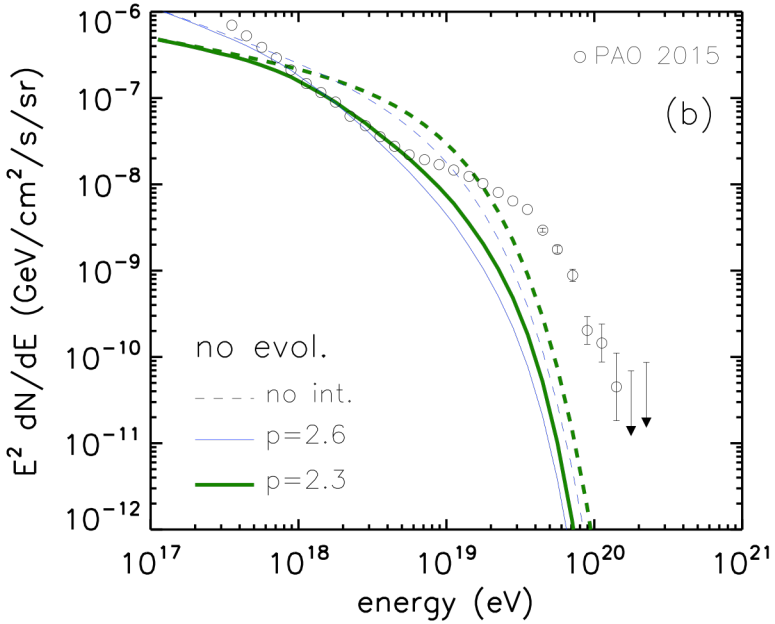

Liu et al., Phys.Rev.D 94 043008 (2016)

The Origin of Protons Below the Ankle

SFR evolution scenario

no evolution scenario

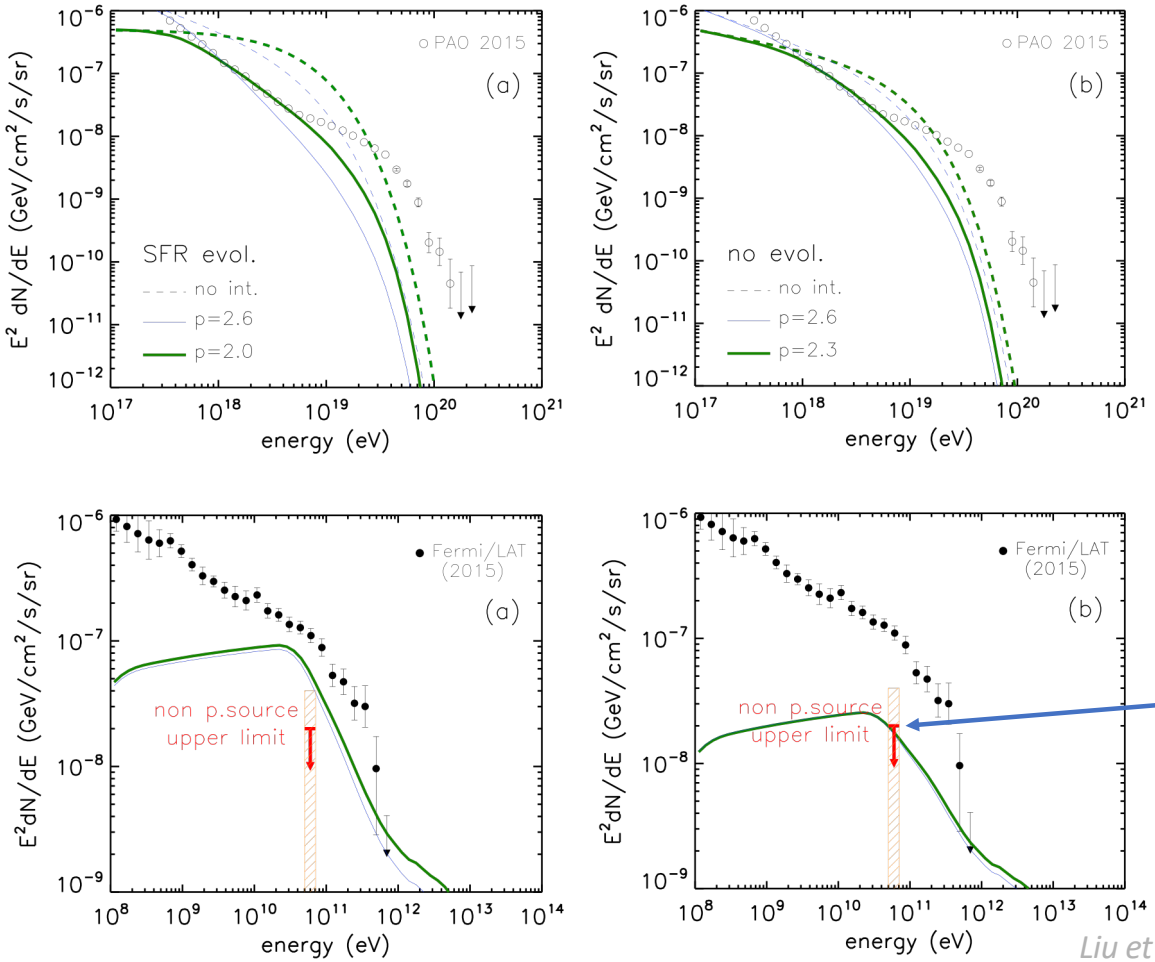

Note- IGRB contribution from cascade losses rather independent of source spectra

New upper limit once (resolved and unresolved) points sources removed

Liu et al., Phys.Rev.D 94 043008 (2016)

The Halo Imprint on the Extragalactic CRs

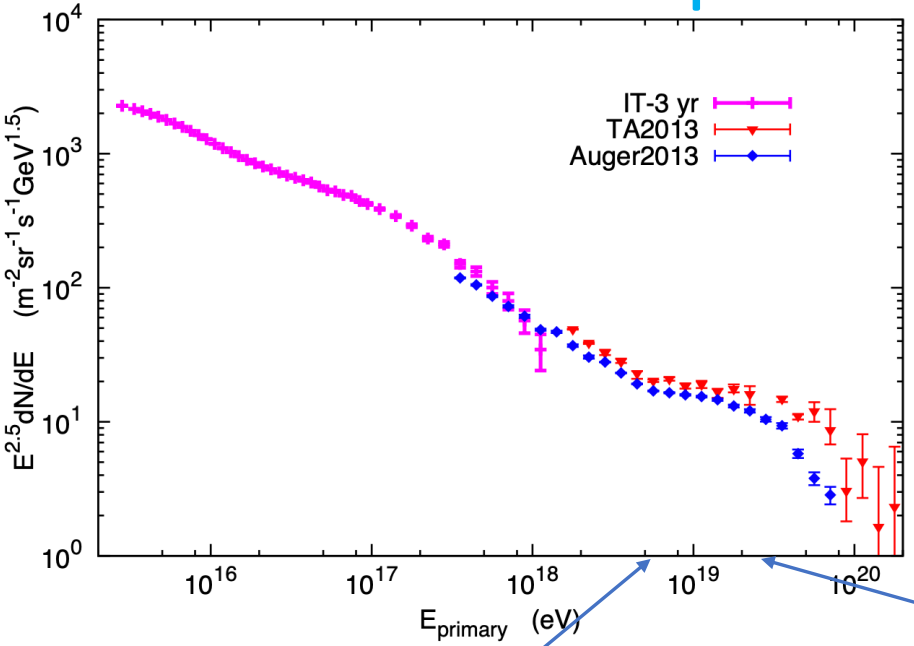

Anisotropy

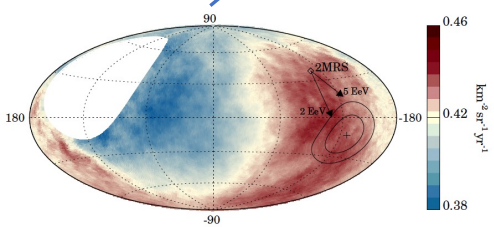

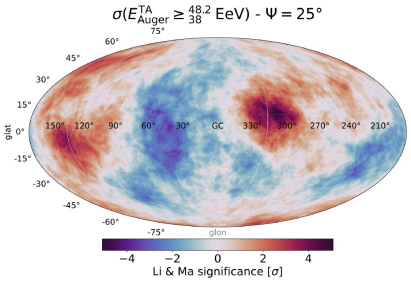

Gupta ApJ, 756 (2012)

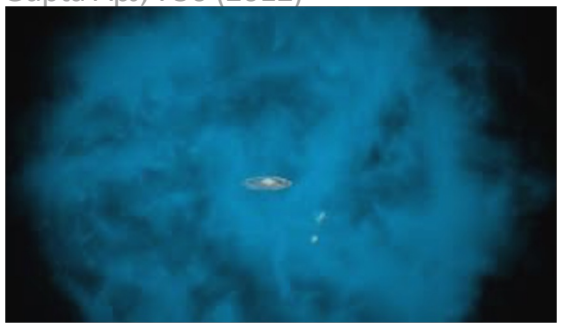

Auger Coll., Science Vol 357, Iss. 6357 1266-1270 (2017)

Caccianiga et al., Auger & TA Coll. PoS (ICRC2023) 521

Large Thermal Pressure in Galactic Haloes

Large Hot Halo

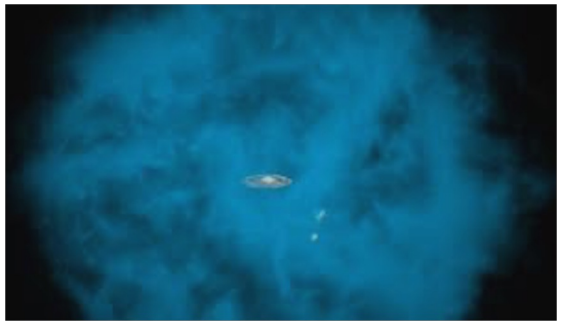

Gupta ApJ, 756 (2012)

X-ray emission

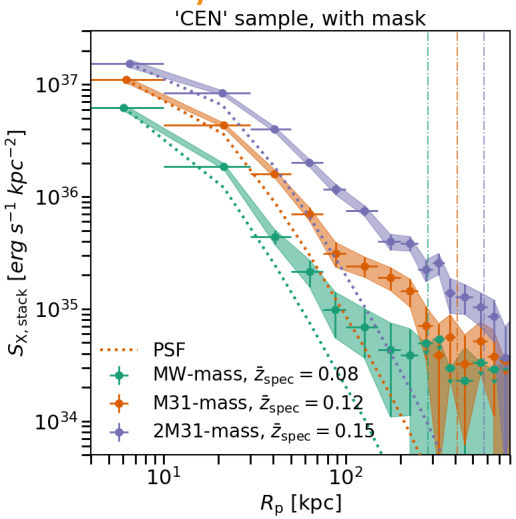

$\mathbf{kT = 0.4\ keV}$

$\mathbf{n(100kpc) \approx 10^{-4} cm^{-3}}$

Faerman ApJ, 893 (2020)

$\mathbf{B(100\ kpc) \approx 0.2\ \mu G}$

consistent with stacked measurement results:

Heesen A&A, 670 (2023)

$\mathbf{r_L(10\ EV) \approx 50\ kpc}$

Bregman et al. ApJ 928 (2022)
Zhang et al. for the eRosita collaboration- A&A (2024)

What “Arrives” is Not Necessarily What is Observed

Cosmic ray source

Reduced diffusion coefficient inside bubble region

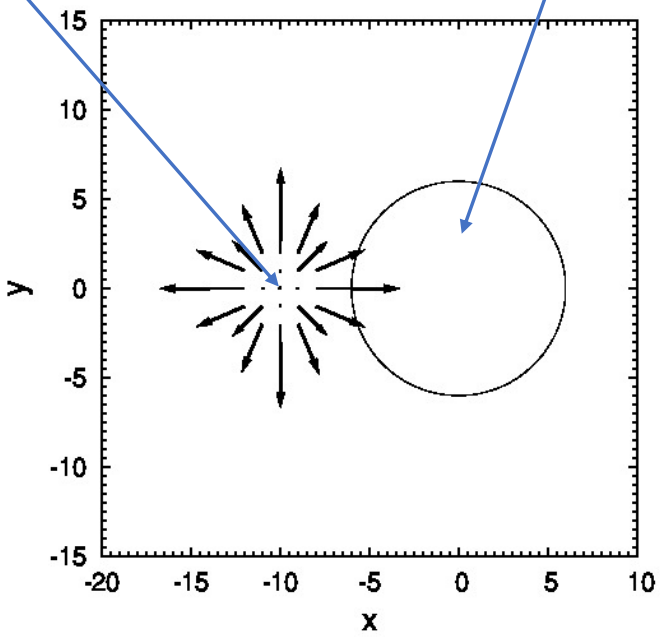

Arrows depict the CR current in different cell regions (D_{out}/D_{in} = 5 adopted for animation)

Injected and Observed Maps

Injected:

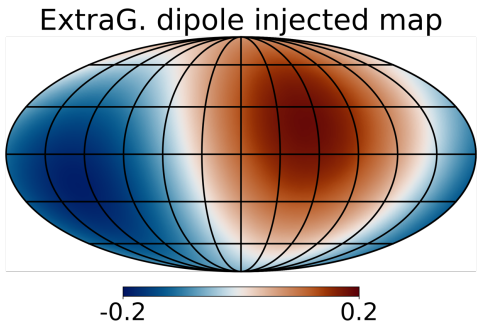

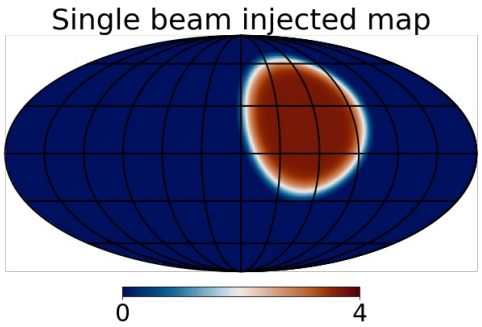

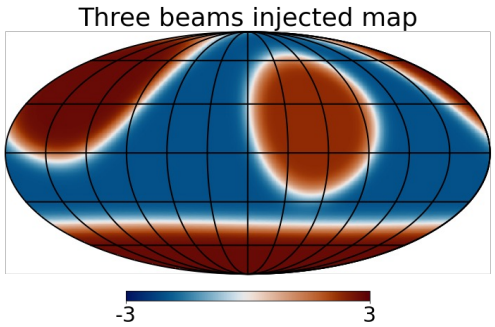

Observed:

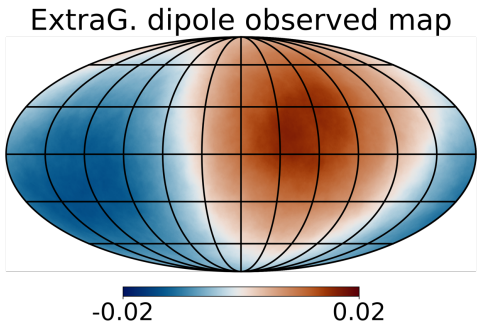

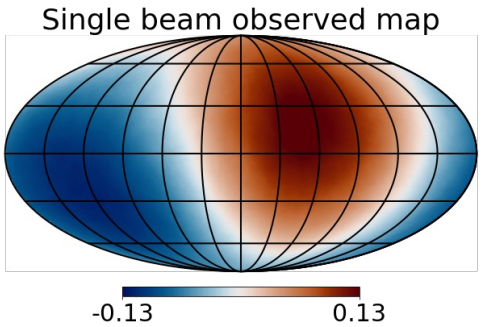

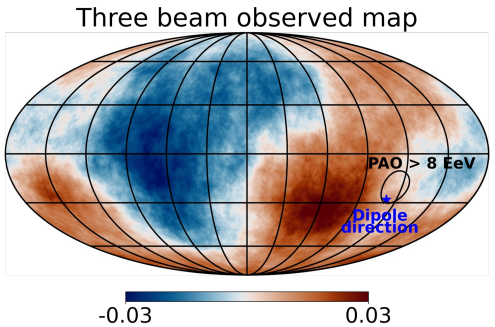

Shaw et al., *MNRAS*, Vol. 543, Iss. 4 (2025)

Power Spectra of Observed Maps

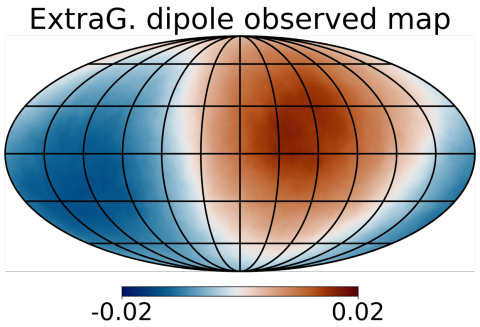

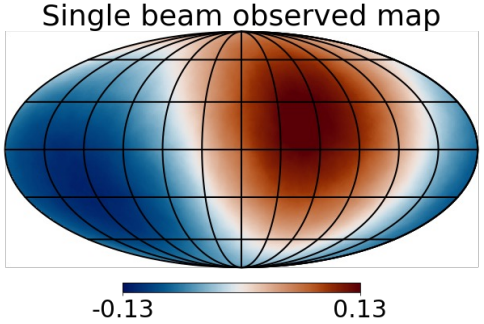

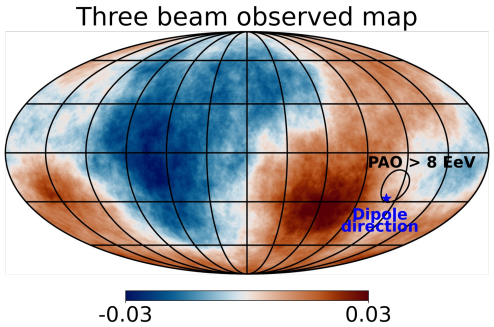

Shaw et al. (in prep.)

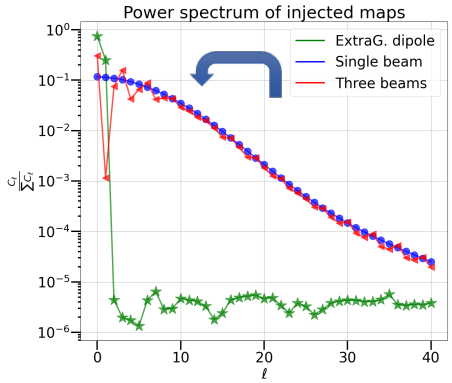

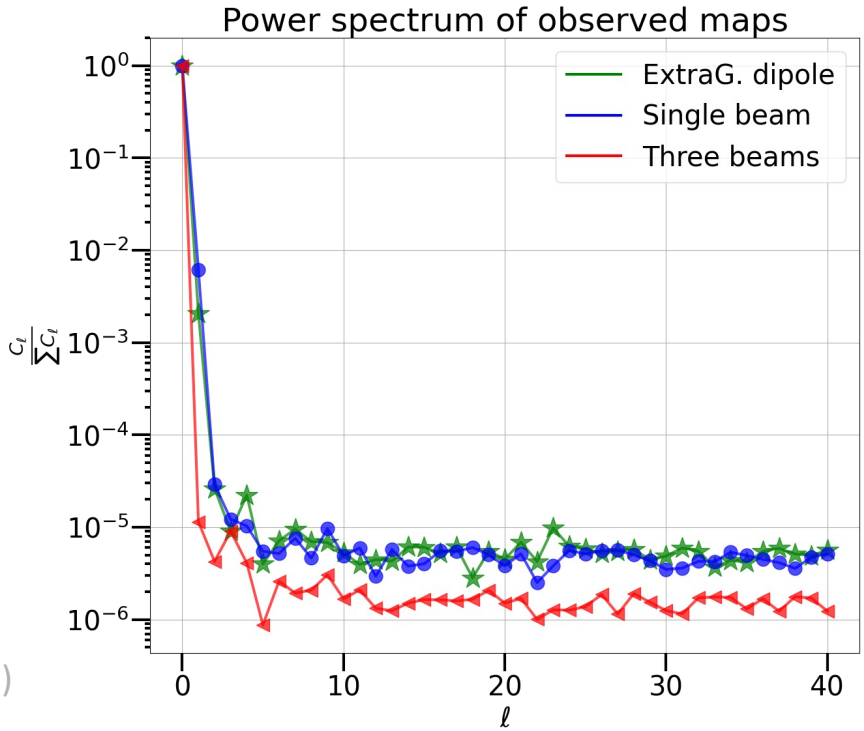

Shaw et al., *MNRAS*, Vol. 543, Iss. 4 (2025)

The Importance of Measuring the Quadrupole Moment at EeV Energies

Shaw et al., *MNRAS*, Vol. 543, Iss. 4 (2025)

Dipole Evolution

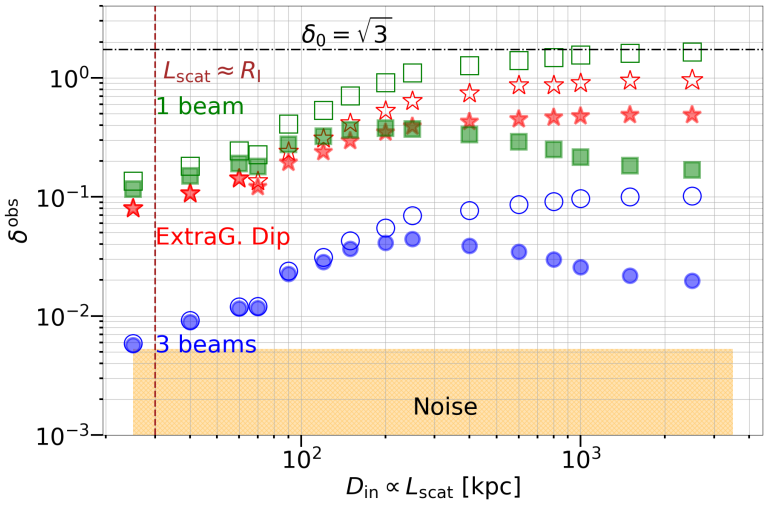

Quadrupole Evolution

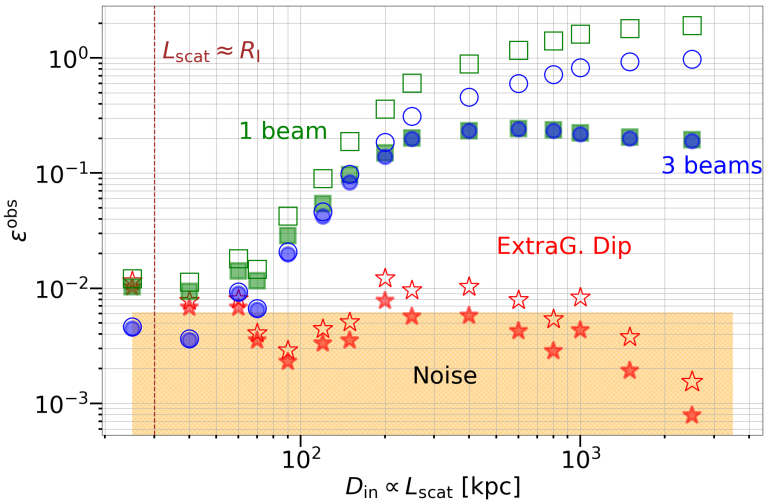

Anisotropy measurements can operate as a Hall probe for measuring the magnetic field characteristics of the halo region

Hall Probe

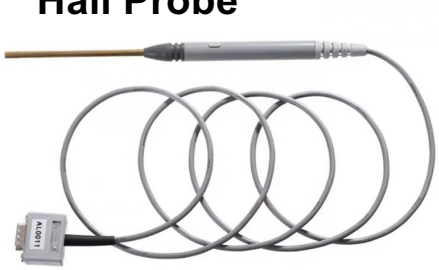

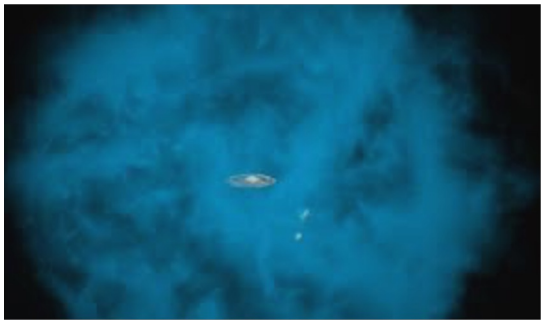

Conclusions

- A Galactic ”Population B” source class seems required, either to bridge knee-ankle gap or (pre)knee-knee gap, and CR composition data allow its E_{max} to be constrained
- The transition to “Population C” (Extragalactic) occurs between 10^{17} eV and $10^{18.5}$ eV, with current data preferring a lower energy transition in this energy range
- New gamma-ray observations are shedding fresh light on “Population B” source candidates
- The “Population C” sources should not have a strong positive source evolution (local?)
- Secondary signatures from CR energy losses in the Galactic halo can be used to probe particle propagation in the halo
- The magnetisation of the Galactic halo can have implications for the penetration of ”Population C” CRs into the halo, which can be tested

What “Arrives” in Not Necessarily What is Observed

Cosmic ray source

Reduced diffusion coefficient inside bubble region

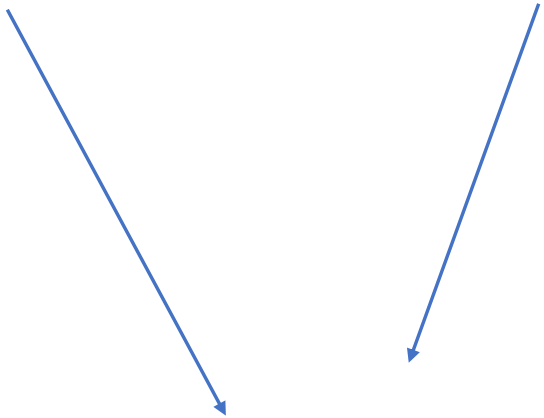

(D_{out}/D_{in} = 5 adopted for animation)

The Fermi/eROSITA Bubbles

- 2 Galactic gamma-ray emitting bubbles exist out to ~8 kpc above and below the Galactic plane
- These appear to be enshrouded in larger hot X-ray emitting bubbles, out to ~14 kpc

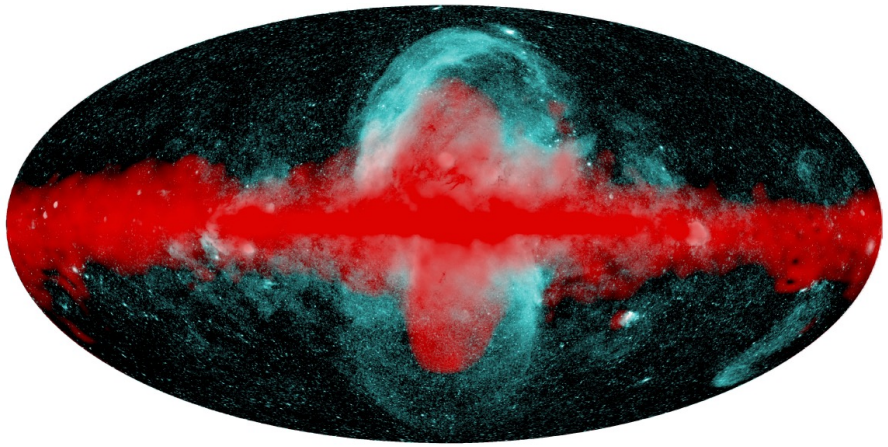

Predehl et al. Nature 588 (2020)

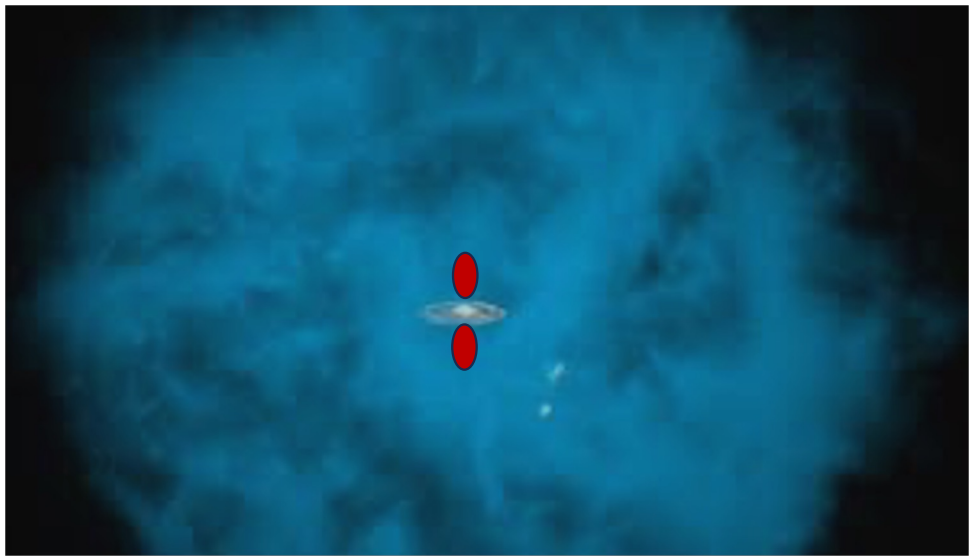

These results appear to indicate that non-thermal particle transport in the Milky Way halo, at least from the Galactic center region, possesses an advective component

Gaisser-Type Population B Candidates: Microquasars

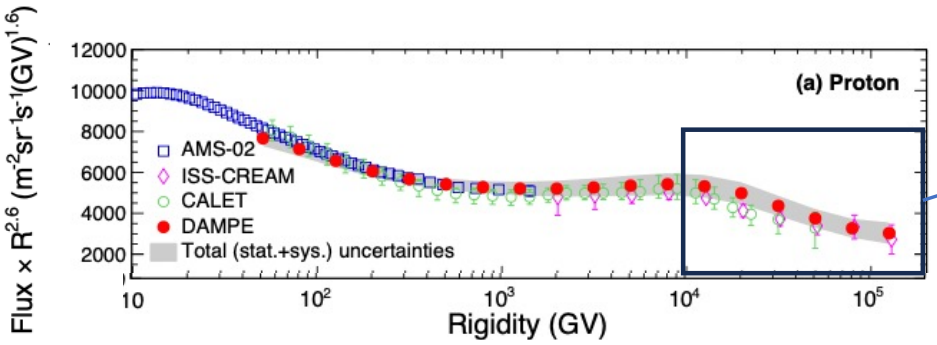

DAMPE Coll. 2511.05409

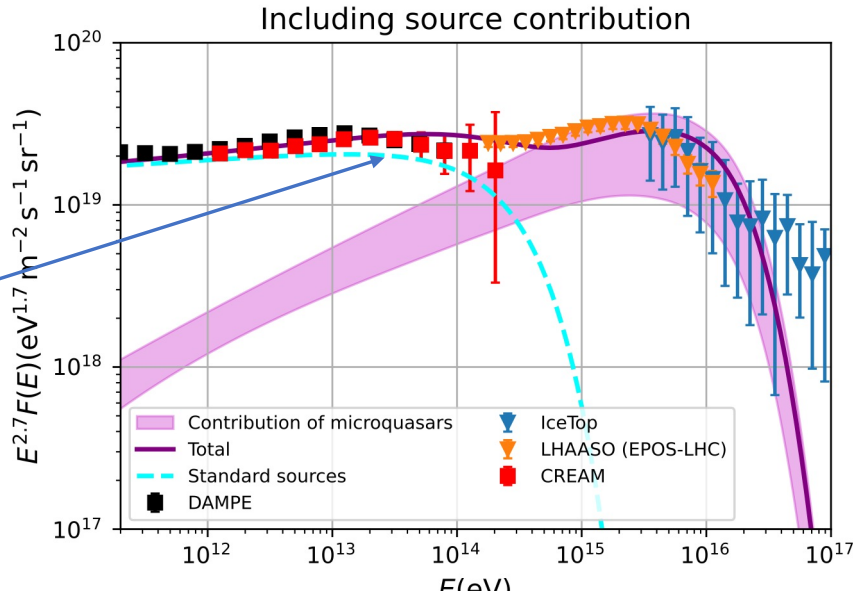

Kaci et al., 2510.01369

$$\mathbf{E_{max} < 2PeV \left(\frac{L}{10^{38}\ erg\ s^{-1}}\right)^{1/2} \left(\frac{\beta}{0.1}\frac{\eta_B}{0.1}\right)^{1/2}}$$

Neutrinos as a Probe of Origin of Protons Below the Ankle

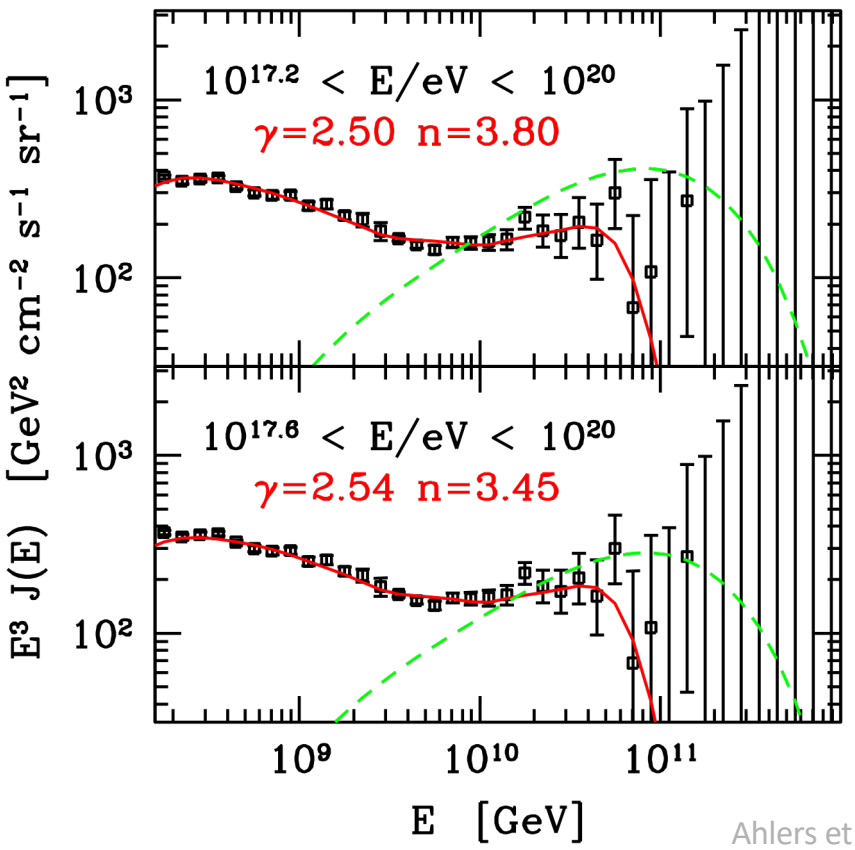

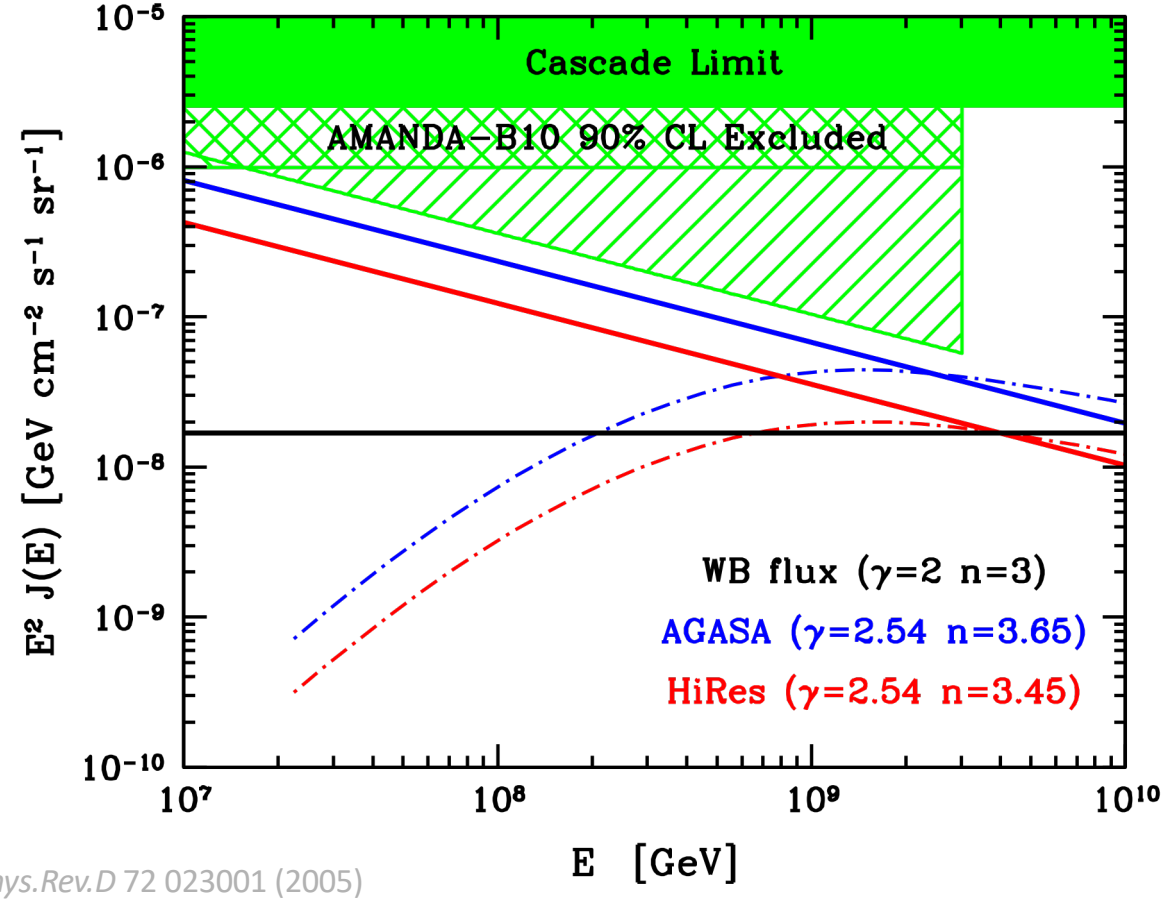

Ahlers et al. *Phys.Rev.D* 72 023001 (2005)

Ahlers et al. *Phys.Rev.D* 79 083009 (2009)

Thermally Driven Outflows: 1/r (Point Source) Potential

Mass Continuity

$$\frac{\partial \rho}{\partial t} + \nabla \cdot (\rho \mathbf{v}) = S_\rho \quad \Rightarrow \quad \rho \mathbf{v} \mathbf{r}^2 = \mathbf{const.}$$

Momentum Continuity

$$\frac{\partial \rho \mathbf{v}}{\partial t} + \nabla \cdot (\rho \mathbf{v}\mathbf{v} + p\mathbf{I}) = -\rho \nabla \Phi_{\mathrm{eff}}$$

For a spherically symmetric (isothermal) thermally driven outflow

$$\Rightarrow \quad \frac{1}{v}\frac{dv}{dr} = \frac{1}{r}\left(\frac{2c_s^2 - r\frac{d\Phi}{dr}}{v^2 - c_s^2}\right)$$

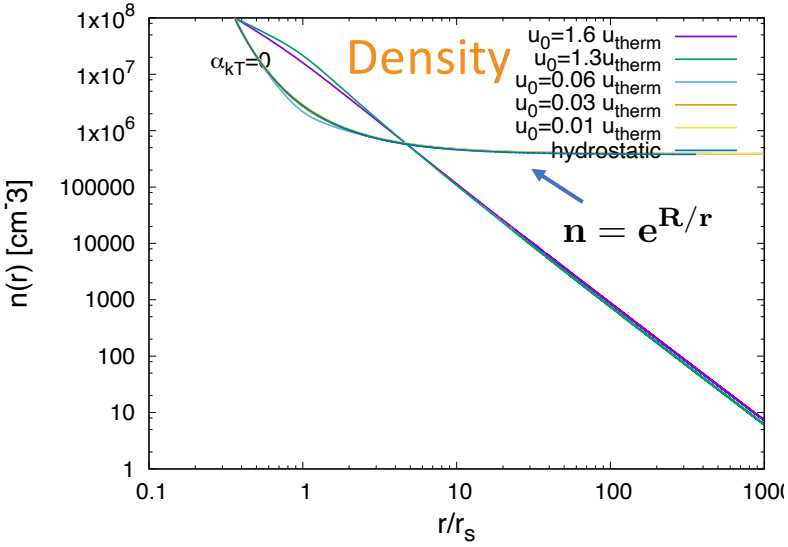

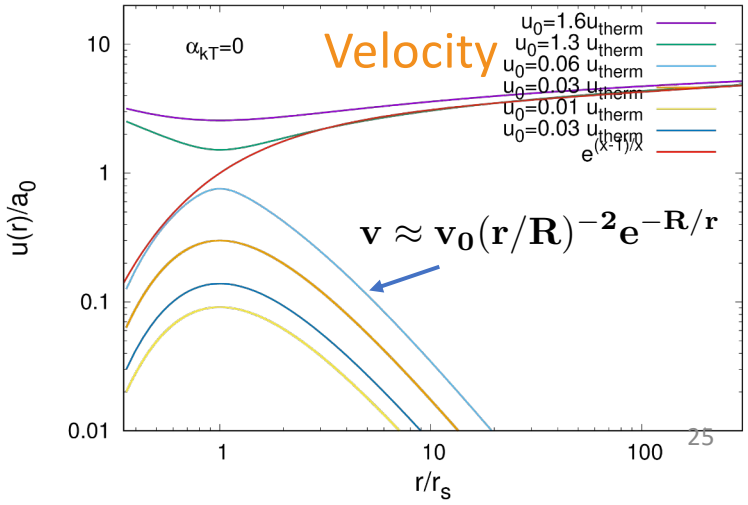

Why Consider Slow Outflows?

Although King function was adopted in eROSITA analysis, result is also consistent with hydrostatic equilibrium expectations for hot gas

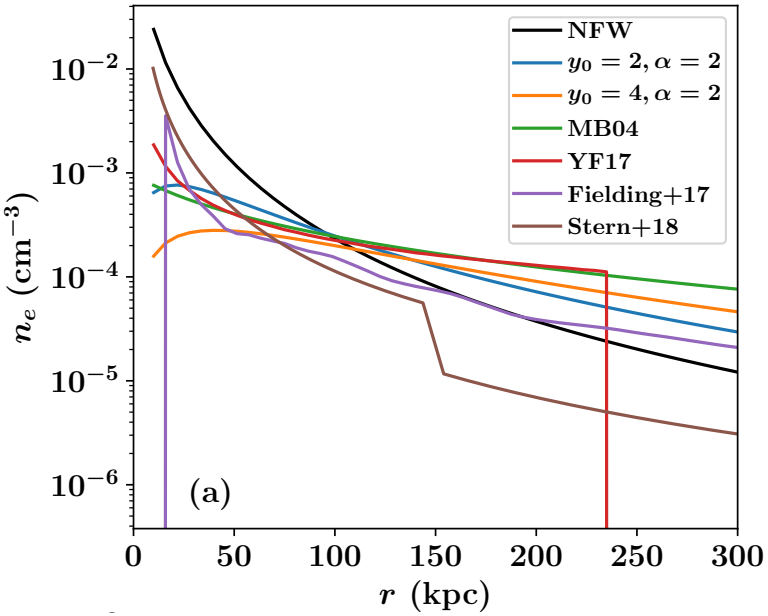

Prochaska et al. MNRAS 485 (2019)

These profiles are consistent with expectations of the halo gas being in hydrostatic equilibrium

$$\mathbf{n = n_0 e^{-\frac{\Phi}{c_s^2}}}$$

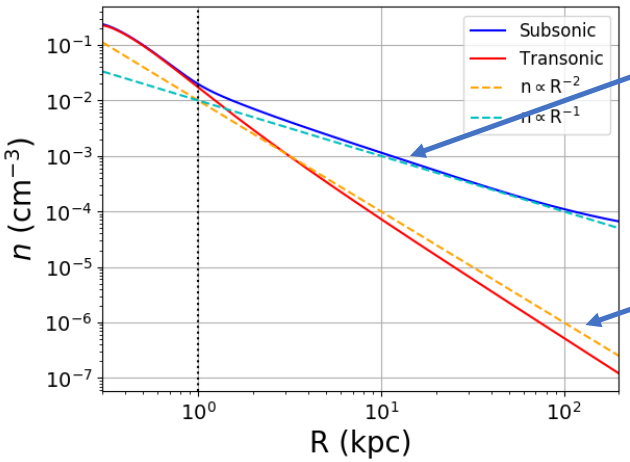

Hydrostatic equilibrium scenario,

$\mathbf{n \propto r^{-1}}$

Supersonic wind scenario,

$\mathbf{n \propto r^{-2}}$

Power Spectra of Injected Maps

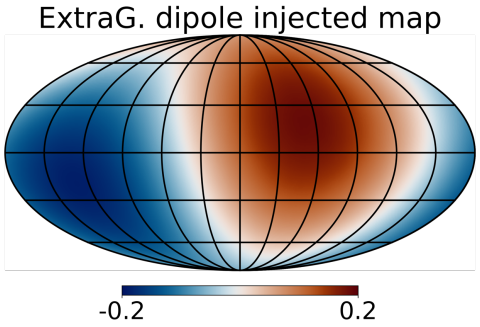

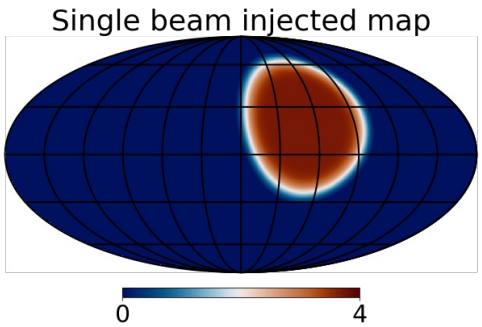

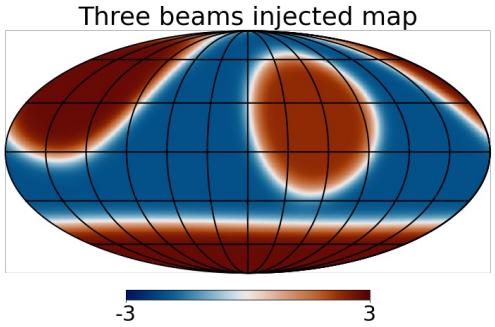

$$\mathbf{\Phi_l} = \int_{-1}^{1} \mathbf{d}\cos\theta \frac{\mathbf{dN}}{\mathbf{N d}\cos\theta} \frac{\mathbf{2l+1}}{\sqrt{\mathbf{2}}} \mathbf{P_l}(\cos\theta)$$

$$\mathbf{C_l} = \frac{\mathbf{\Phi_l^2}/(\mathbf{2l+1})}{\sum_{\mathbf{n}} \mathbf{\Phi_n}/(\mathbf{2n+1})}$$

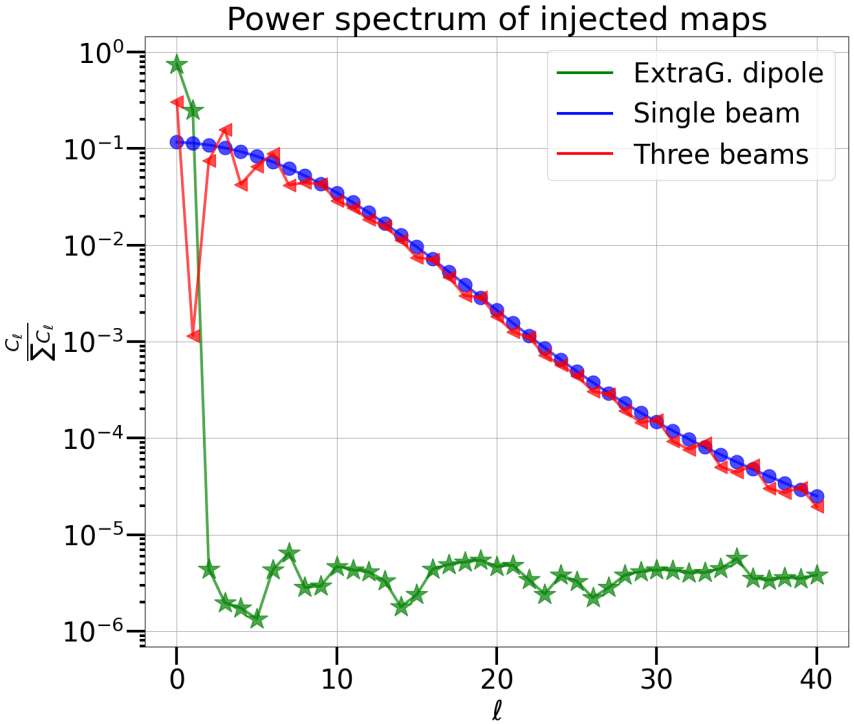

Shaw et al., *MNRAS*, Vol. 543, Iss. 4 (2025)

Are there Secondary Signatures of Galactic CR in the Galactic Halo Environment?

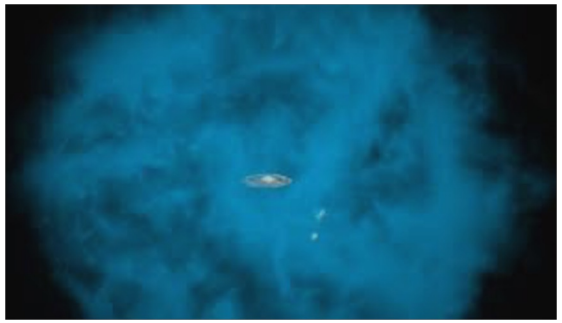

The Fermi/eROSITA Bubbles

- 2 Galactic gamma-ray emitting bubbles exist out to ~8 kpc above and below the Galactic plane
- These appear to be enshrouded in larger hot X-ray emitting bubbles, out to ~14 kpc

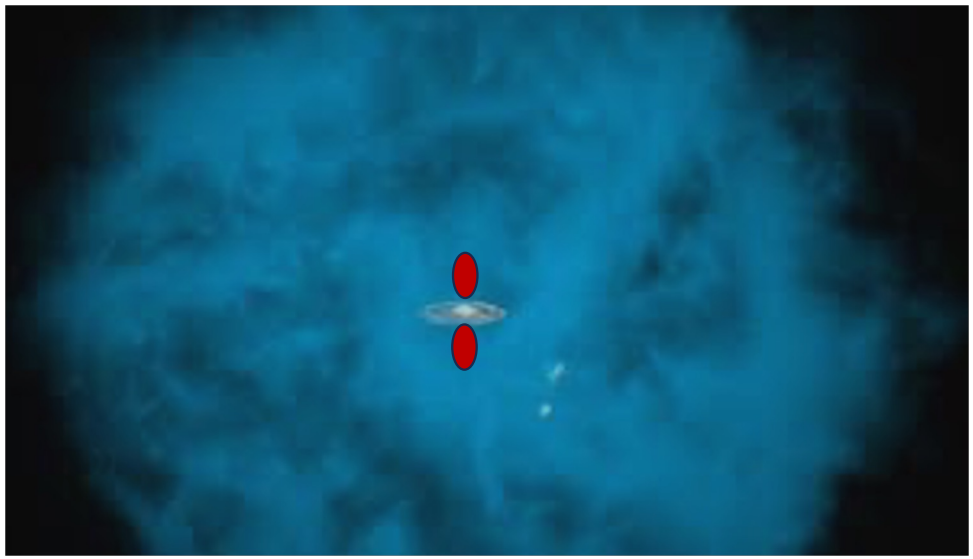

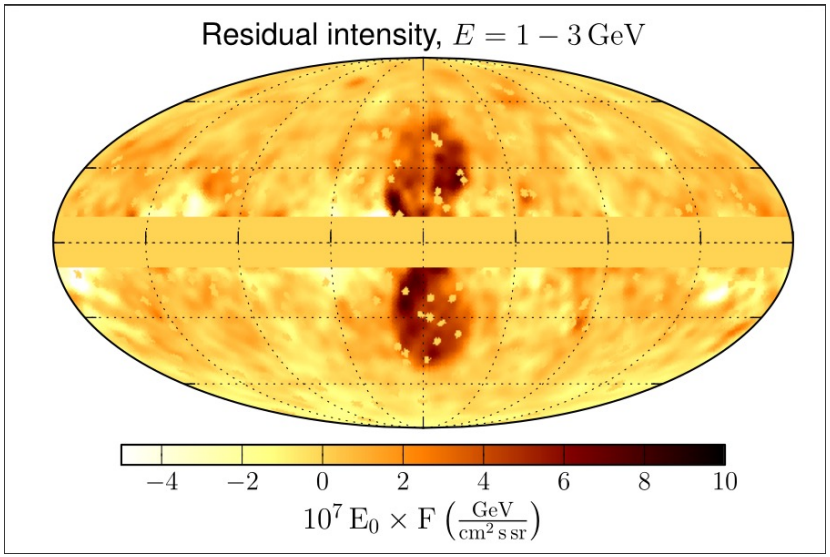

Ackermann et al. ApJ 793 (2014)

These results appear to indicate that non-thermal particle transport in the Milky Way halo, at least from the Galactic center region, possesses an advective component

Large Thermal Pressure in Galactic Haloes

X-ray observations of bright AGN indicate the presence of a hot local absorber.

Large Hot Halo

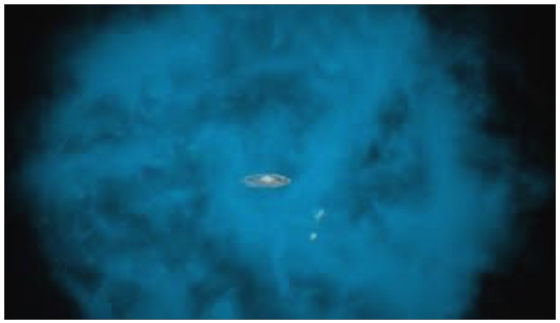

Gupta ApJ, 756 (2012)

$$\mathbf{M} = (\mathbf{0.8 - 3.5}) \times \mathbf{10^{11}}\ \mathbf{M_\odot}$$

Zhang et al., 2511.17313

King function

$$\mathbf{n} = \mathbf{n_0}\left[\mathbf{1} + \left(\frac{\mathbf{r}}{\mathbf{r_c}}\right)^{\mathbf{2}}\right]^{-\frac{\mathbf{3}}{\mathbf{2}}\beta}$$

$$\beta \approx \mathbf{0.4 \pm 0.1}$$

$$\mathbf{n} \propto \mathbf{r}^{\mathbf{-1}}$$

More recently, the ram pressure stripping of satellite galaxies + emission from the hot absorber have been collectively used to probe the halo gas density.

Ram pressure stripping

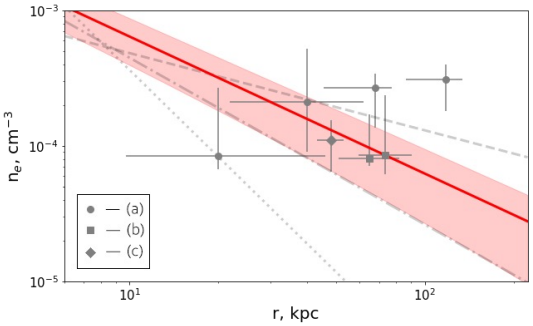

Faerman ApJ 835 (2017), Martynenko MNRAS, 511 (2022)

X-ray emission

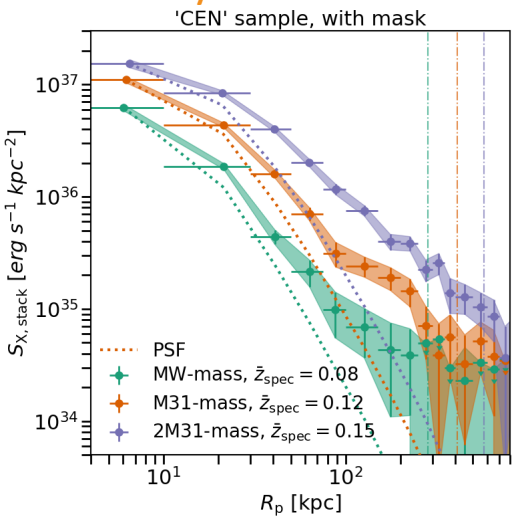

Bregman et al. ApJ 928 (2022)
Zhang et al. for the eRosita collaboration- A&A (2024)

Inputs for Hydrodynamical Simulations

The Galactic potential

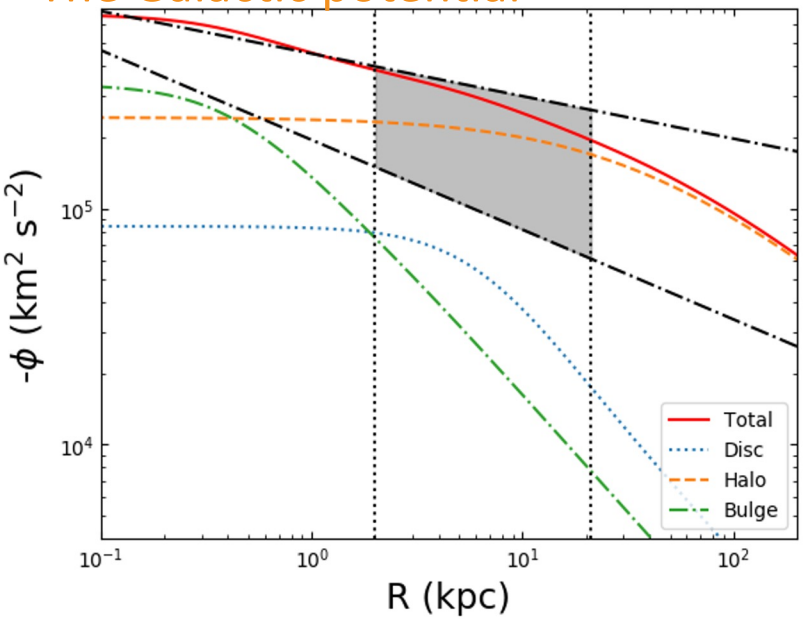

Tourmente et al. *MNRAS*, Vol 518, Iss. 4, (2023)

$$\mathbf{n = n_0 e^{-\frac{\Phi}{c_s^2}}}$$

Gas Density Distribution

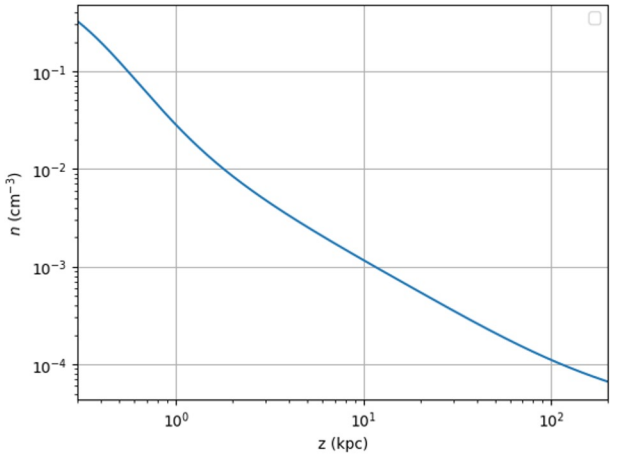

Thermal gas temperature

Isothermal temperature distribution adopted

$$\mathbf{kT = 0.4\ keV}$$

- For hydrodynamical simulations, gas density was started off with a hydrostatic equilibrium distribution
- Assumed a heating process exists throughout the simulation volume that keeps the gas hot (with an isothermal temperature)

Inputs for Hydrodynamical Simulations

The Galactic potential

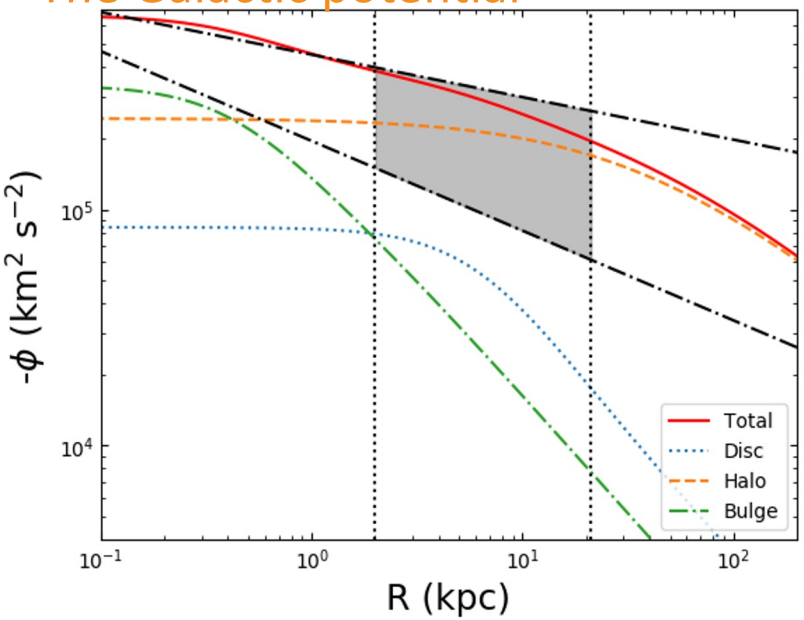

$$\mathbf{n = n_0 e^{-\frac{\Phi}{c_s^2}}}$$

Gas Density Distribution

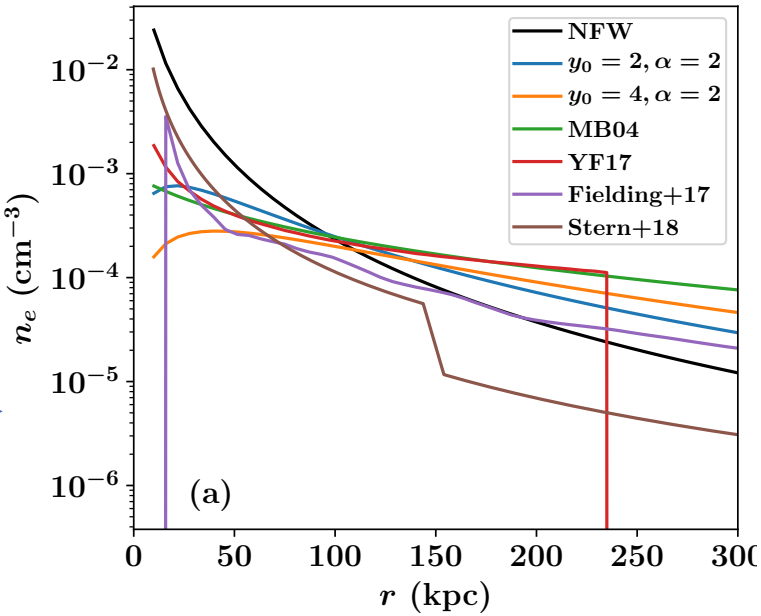

Prochaska et al. MNRAS 485 (2019)

Thermal gas temperature

Isothermal temperature distribution adopted

$$\mathbf{kT = 0.4\ keV}$$

- For hydrodynamical simulations, gas density was started off with a hydrostatic equilibrium distribution
- Assumed a heating process exists throughout the simulation volume that keeps the gas hot (with an isothermal temperature)

Subsonic Outflow Result for Isothermal Gas Using PLUTO

Resultant 2D velocity field simulation

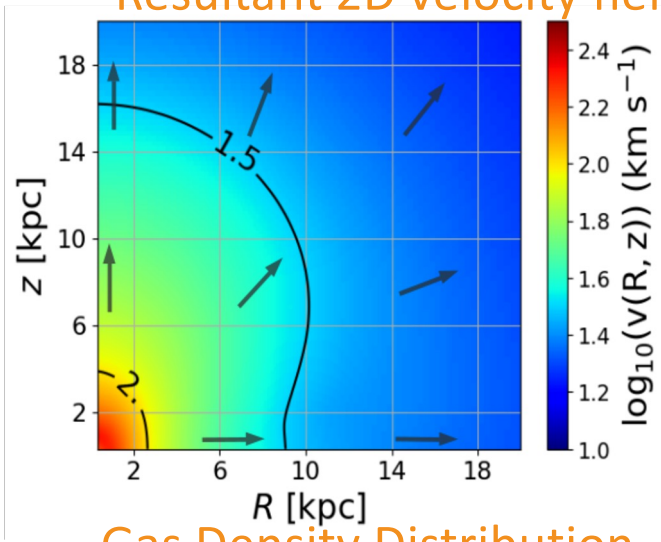

Tourmente et al. *MNRAS*, Vol 518, Iss. 4, (2023)
Tourmente et al., 2507.20893

velocity profile

Galactic center source

$$\frac{\partial f}{\partial t} = \nabla \cdot (D\nabla f - \mathbf{v}f) + \frac{1}{p^2}\frac{\partial}{\partial p}\left[(\nabla \cdot \mathbf{v})\frac{p^3}{3}f\right] - \frac{f}{\tau_{\text{loss}}} + \frac{Q}{p^2}$$

halo gas

Gas Density Distribution

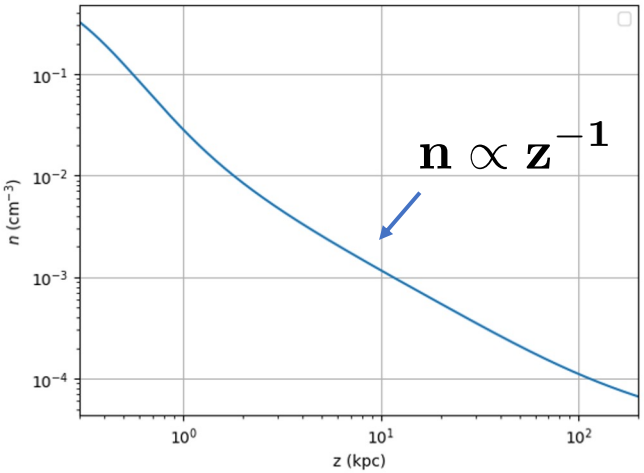

Simulation results assuming constant source injection term present at the Galactic center

Gamma-Ray Skymap

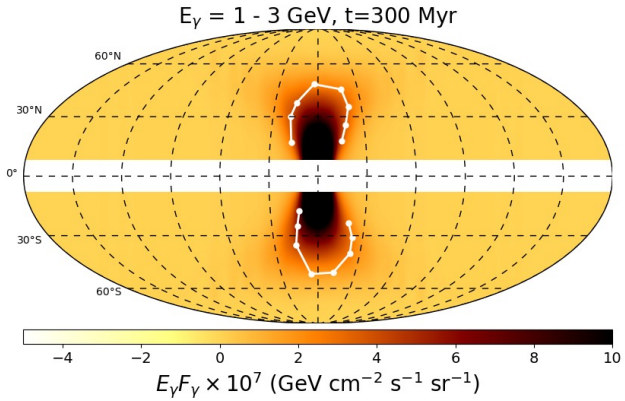

Secondary to Primary Cosmic Rays as a Probe of Galactic Halo Size (B/C)- LIMITATIONS

$$\frac{\partial f}{\partial t} = \nabla \cdot (D \nabla f - \mathbf{v} f) + \frac{1}{p^2}\frac{\partial}{\partial p}\left[p^2 \left\langle \frac{D_{pp}}{p^2} \right\rangle \frac{\partial f}{\partial p} - \left\langle (\nabla \cdot \mathbf{v}) \frac{p^3}{3} \right\rangle \frac{\partial f}{\partial p} \right] - \frac{f}{\tau_s} + \frac{Q}{p^2}$$

(thanks for C. Li for preparing these plots!)

Thanks to C. Li for these plots

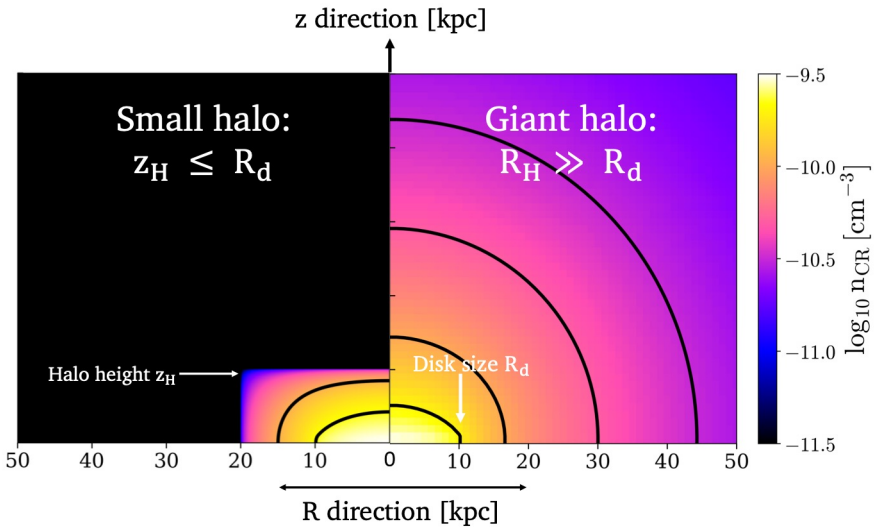

Hopkins et al, MNRAS 516 (2022) 3, 3470-3514

….the “halo size” does not really represent the scale-length of e.g. the magnetic energy or free-electron density profile; rather, the “halo size” in these models is more accurately defined as the volume interior to which CRs have an order-unity probability of scattering “back to” the Solar position.

Shizuo Kakutani

“A drunk man will eventually find his way home, but a drunk bird may get lost forever.”

Secondary to Primary Cosmic Rays as a Probe of Galactic Halo Size (B/C)- LIMITATIONS

$$\frac{\partial f}{\partial t} = \nabla \cdot (D \nabla f - \mathbf{v} f) + \frac{1}{p^2} \frac{\partial}{\partial p} \left[(\nabla \cdot \mathbf{v}) \frac{p^3}{3} \right] - \left(\frac{1}{\tau_s} \right) + \frac{Q}{p^2}$$

Thanks to C. Li for these plots
Hopkins et al, MNRAS 516 (2022) 3, 3470-3514

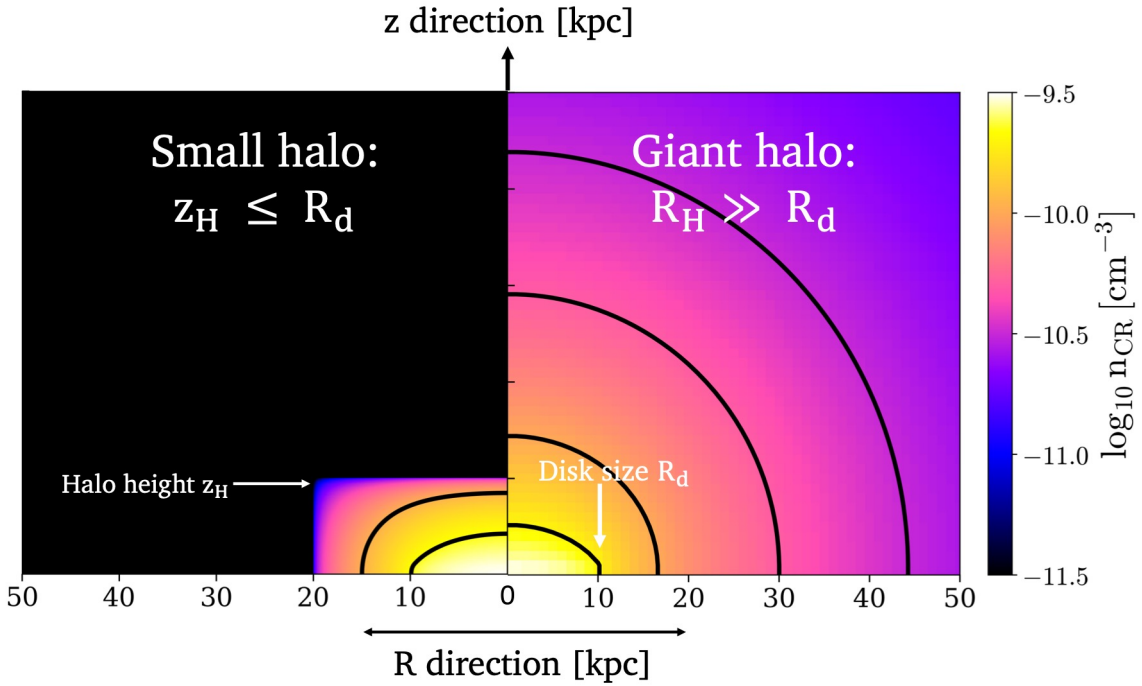

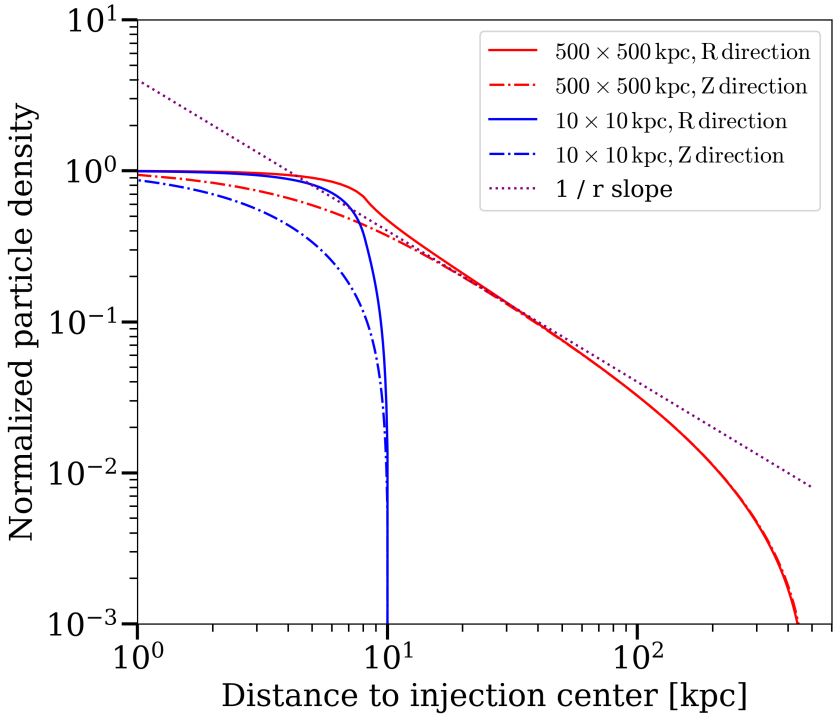

Neutrino Emission from the Galactic Halo?

CR Distribution

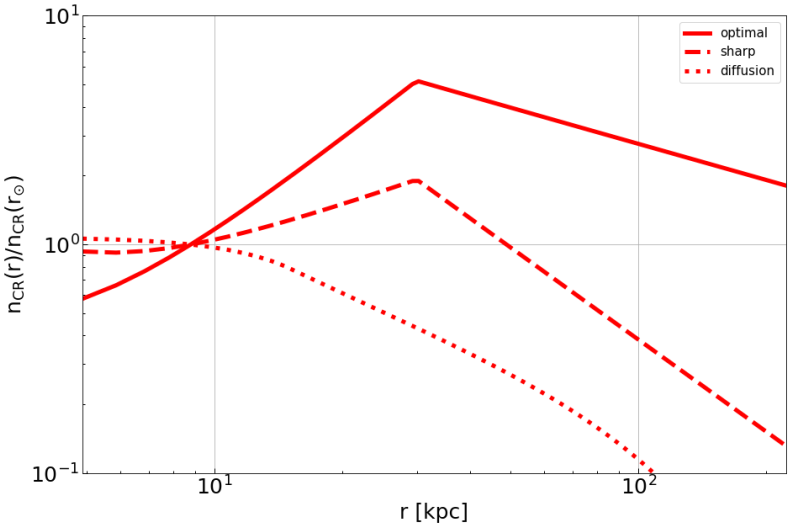

Kalashev et al., *JCAP* 03 (2023) 053

Gas Density Distribution

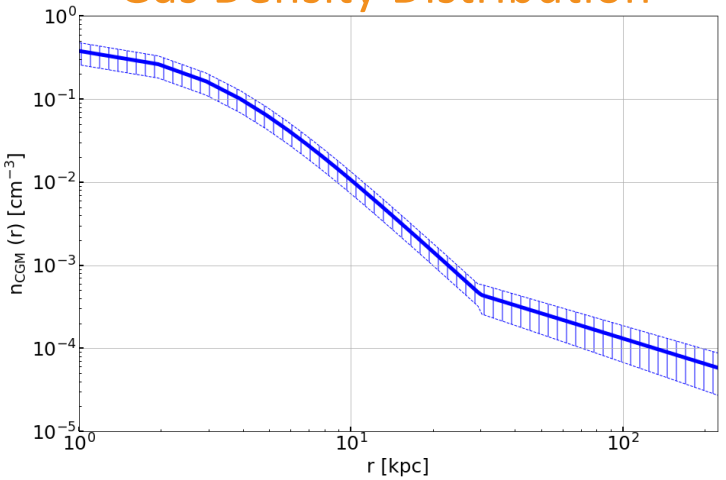

Halo Neutrino Flux (Diffusive Case)

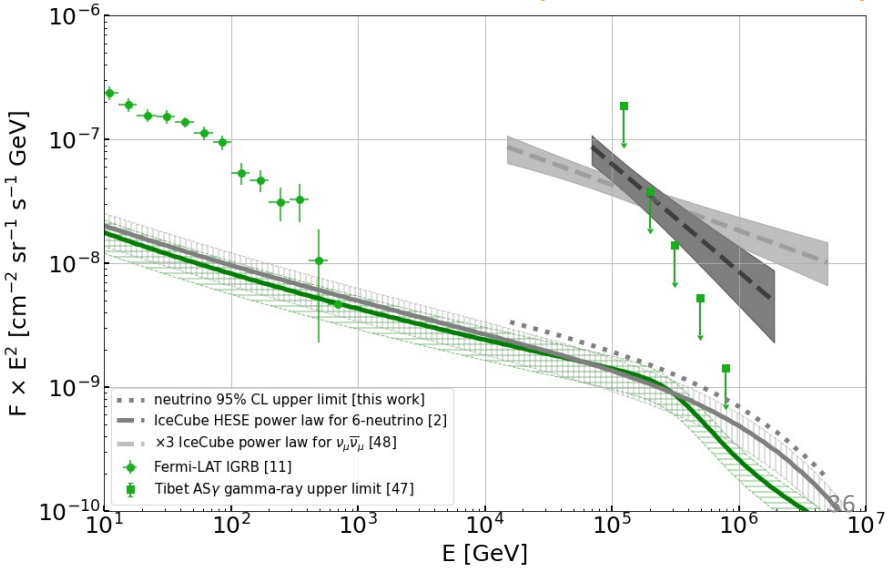

Understanding the CR transport process in the halo is key for these results

In this case, the circumgalactic neutrino flux contribution is comparable with the Galactic-disk contribution.

Probes of CR Escaping Nearby Galactic Haloes

Evidence for Diffuse Gamma-Rays Emission from M31's Galactic Halo

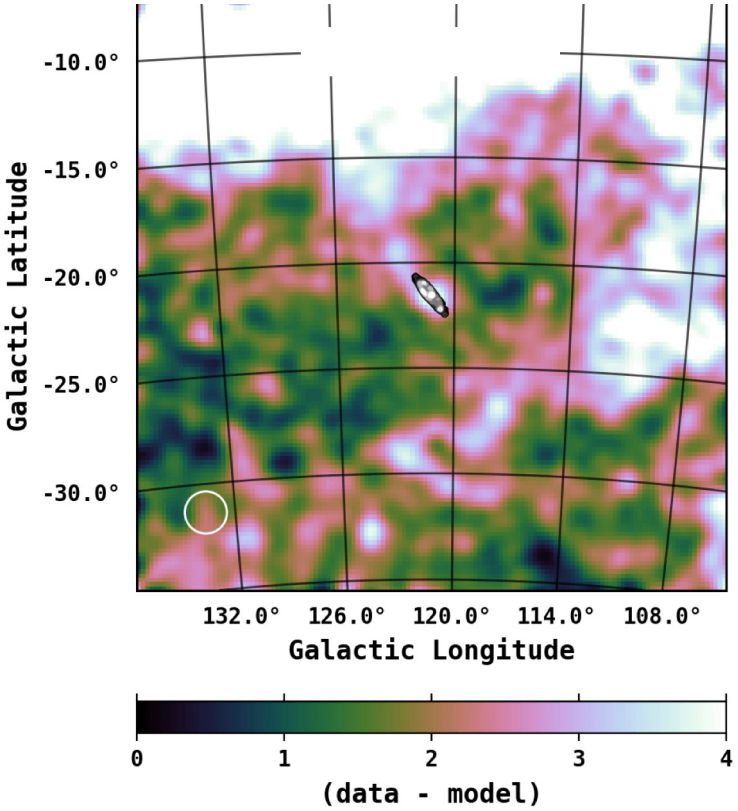

Suggests that emission extends out to tens of degrees (100s kpc)

Evidence that the escape of CRs from the Galaxy is not dictated solely by diffusive transport

Karwin et al., ApJ 880:95 48pp (2019)

Moskalenko paper

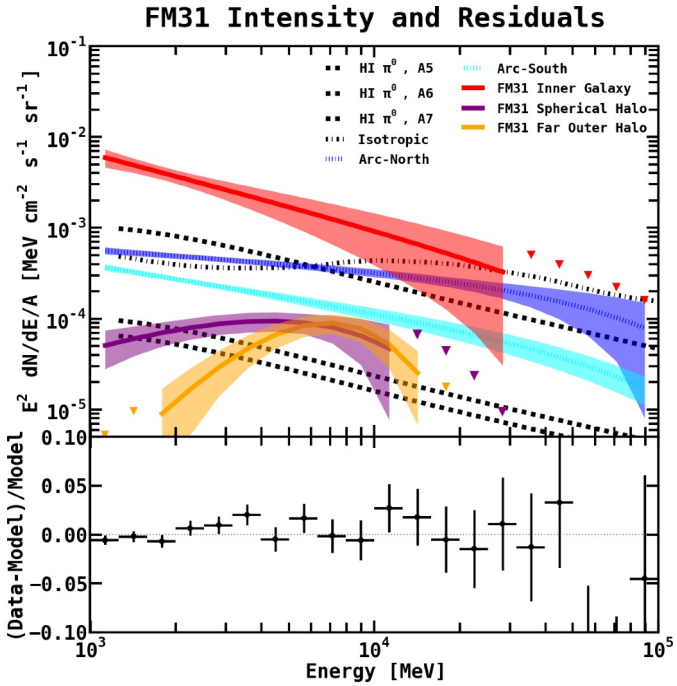

Probes of CR Escaping Nearby Galactic Haloes

Evidence for Diffuse Gamma-Rays Emission from M31's Galactic Halo

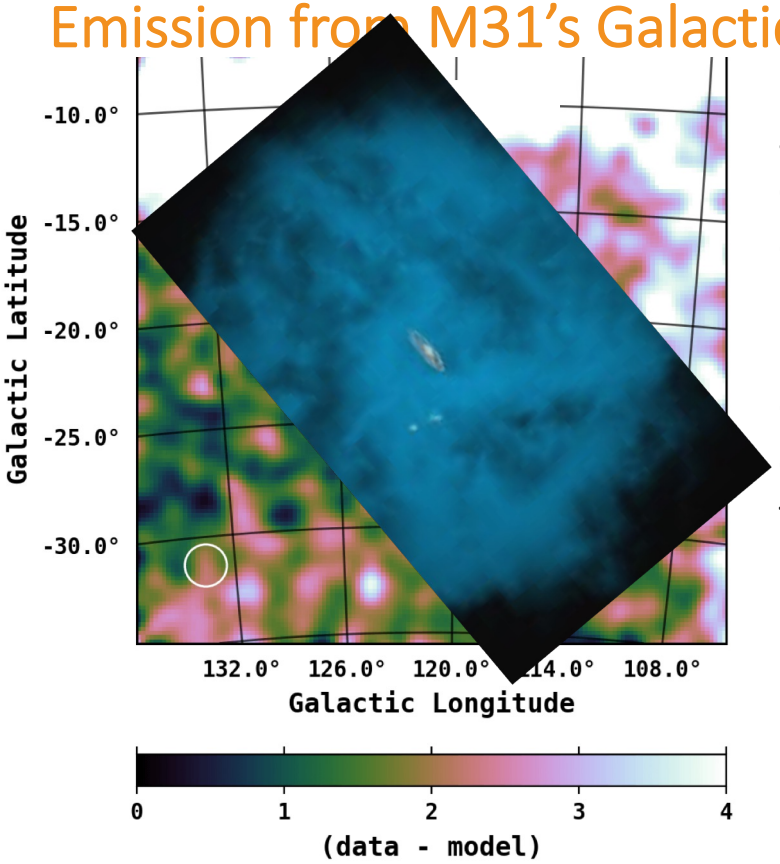

Suggests that emission extends out to tens of degrees (100s kpc)

Evidence that the escape of CRs from the Galaxy is not dictated solely by diffusive transport

Karwin et al., ApJ 880:95 48pp (2019)

Moskalenko paper

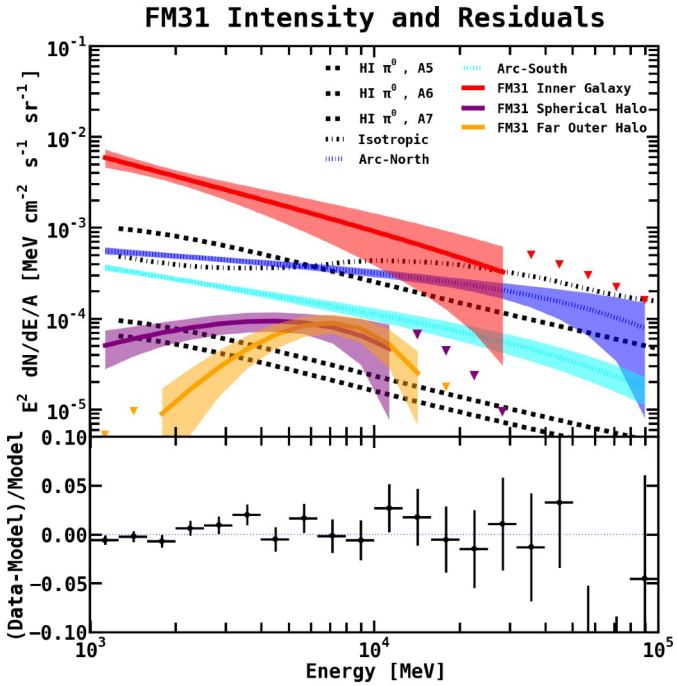

How Might the Galactic Halo Effect The Arrival of “Population C” CR?

“Population C”
CR source

The Importance of Measuring the Quadrupole Moment at EeV Energies

Shaw et al., *MNRAS*, Vol. 543, Iss. 4 (2025)

Transition ”energy” for which halo becomes thin

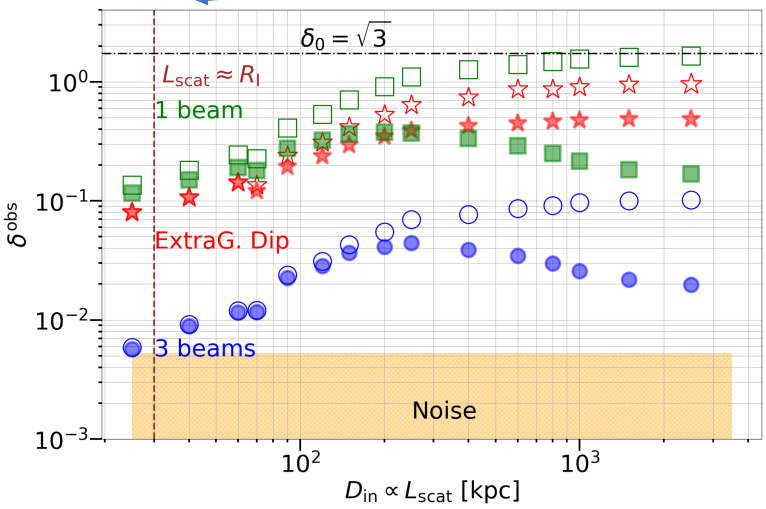

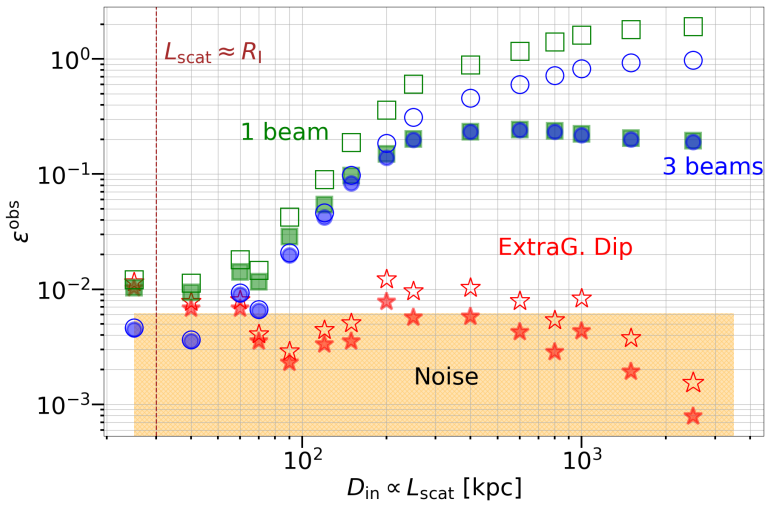

Note the difference in growth rates of dipole and quadrupole amplitude with L_{scat}

Galactic/Extragalactic Cosmic Ray Transition

An Analogy Between

Gaisser, HAP Workshop, KIT (2015)

Heliosphere

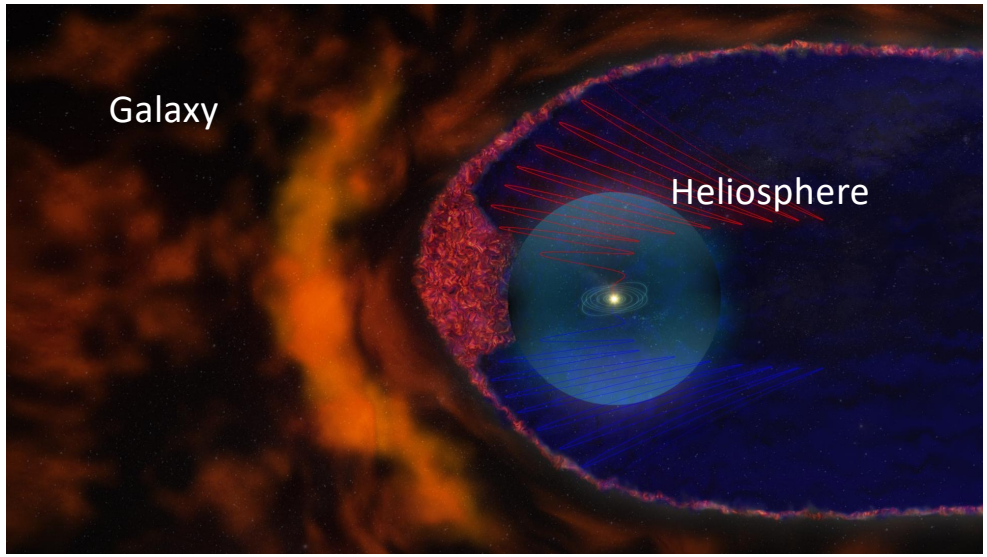

Galactic Halo

Origins of the CR Spectrum?

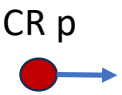

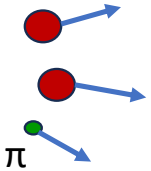

K. Brecher, G. R. Burbidge, ApJ 174 (1972) 253

V. L. Ginzburg, Astro. and Space Phys., Vol. 4, p.167 (1972)

A.W. Strong, *Nucl.Part.Phys.Proc.* 297-299 (2018) 165-170

Back in the 1970s, there was a debate about whether **all** CRs could be extragalactic. Subsequent diffuse gamma-ray observations, however, constrained such a scenario.

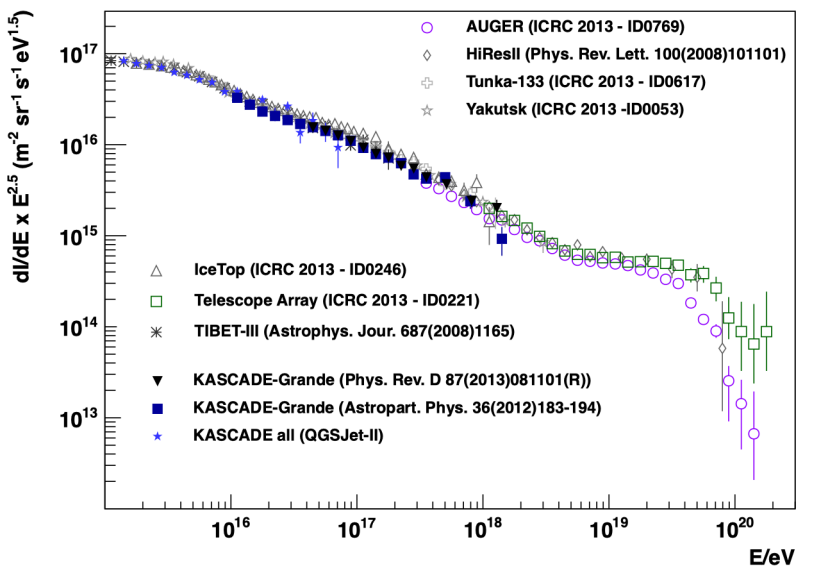

Gaisser, *Front.Phys.(Beijing)* 8 (2013) 748-758

Can Constraints be Placed on Population C?

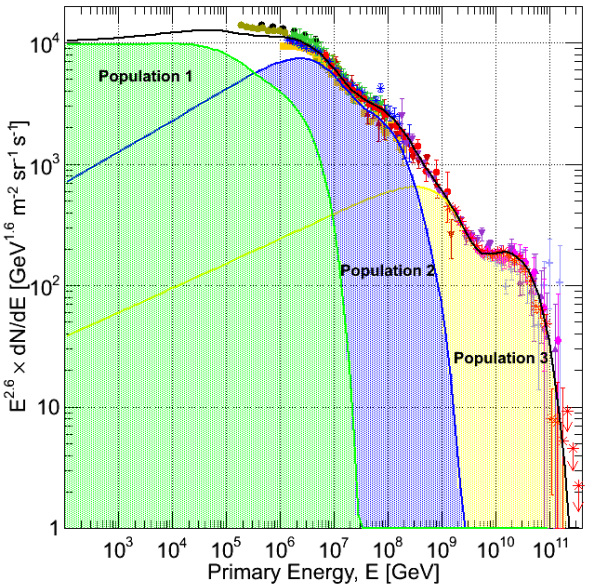

Universality of Cascade Spectra

Aharonian et al., *Astrophys.J.Lett.* 423 (1994) L5-L8
Berezinsky *Phys.Rev.D* 94 (2016) 2, 023007

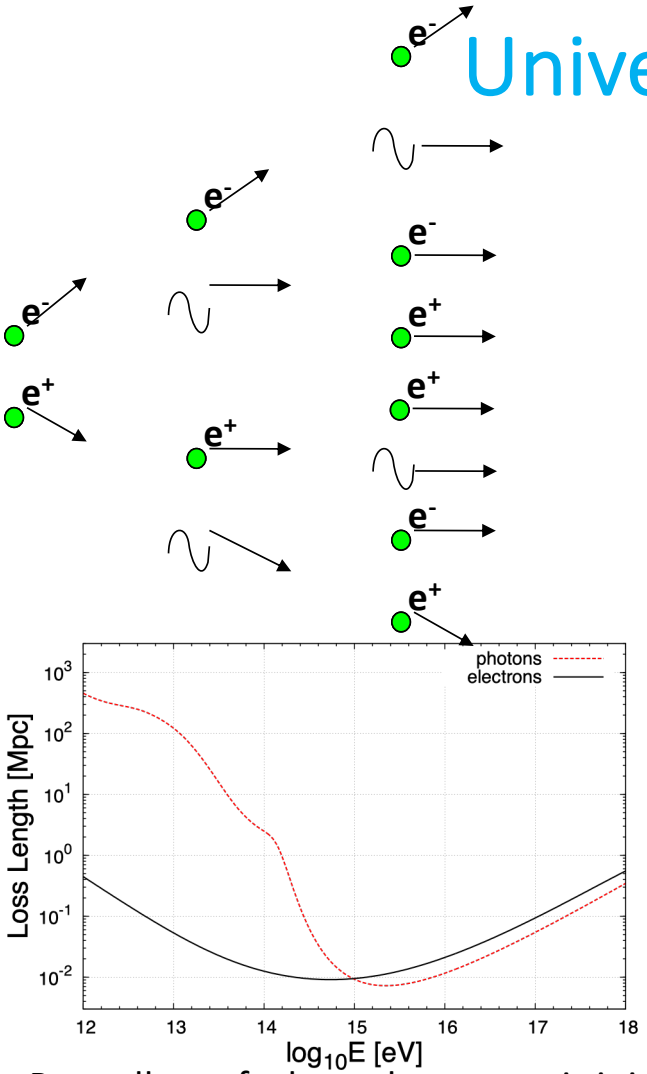

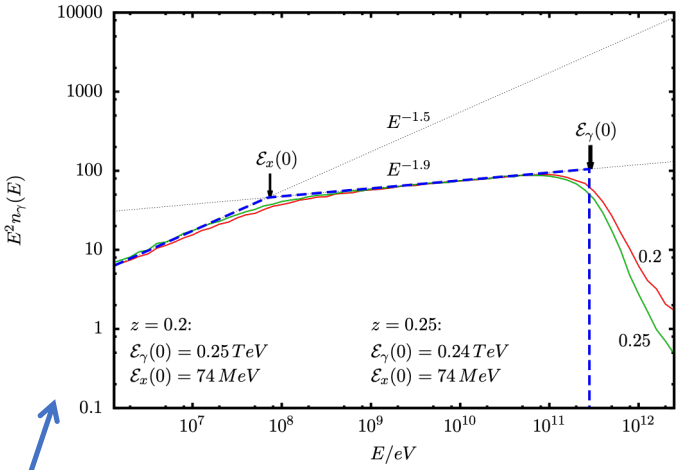

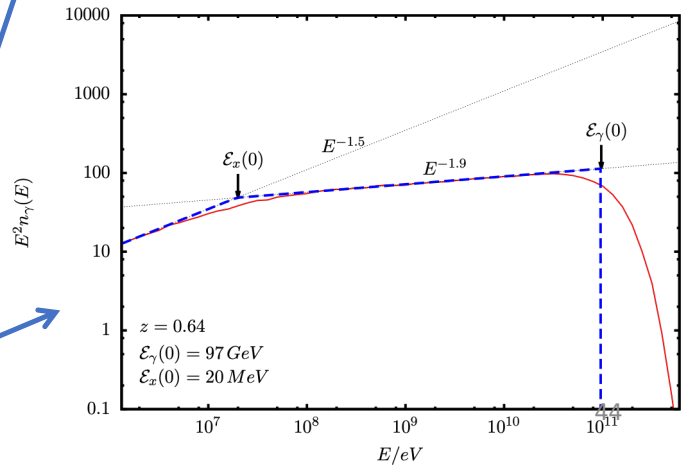

Regardless of where the energy is injected (ie independent of source z), the arriving flux possesses a universal shape

Galactic/Extragalactic Cosmic Rays

An Anology with the Transition from the Heliospheric to Galactic CR Spectrum

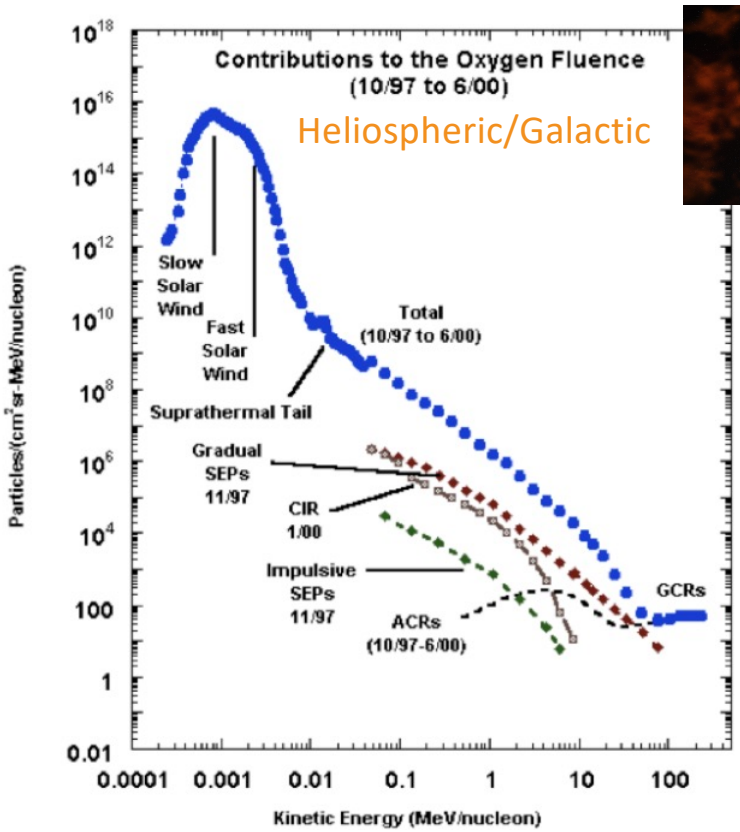

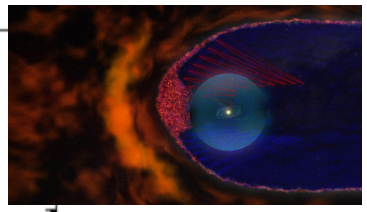

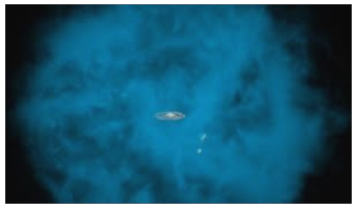

Gaisser, *Front.Phys.(Beijing)* 8 (2013) 748-758

Galactic /Extragalactic

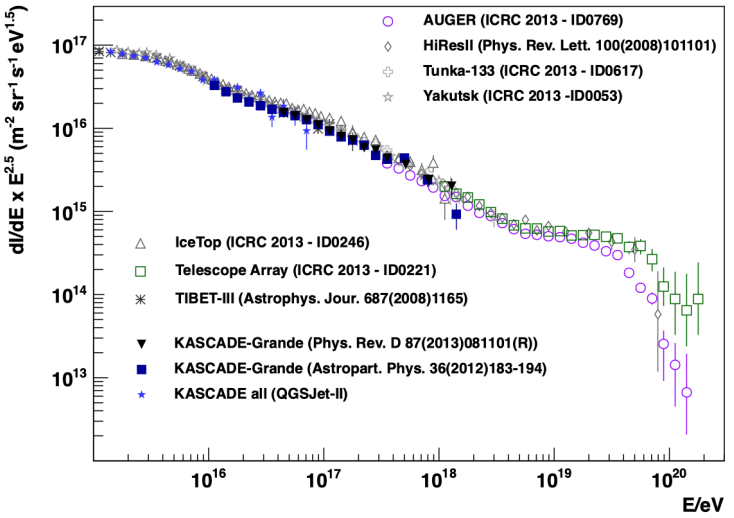

- Several kinds of events contribute
  - Typically power law with exponential cutoff
  - Different values of E_{max}
  - High energy events less frequent
- Overall spectrum is a power-law with a knee

Origins of the CR Spectrum?

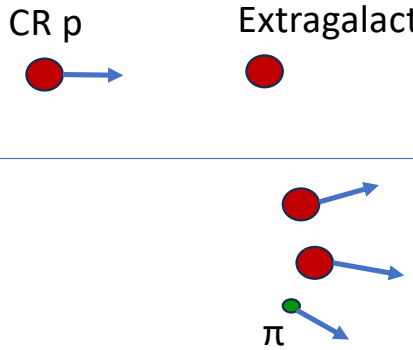

K. Brecher, G. R. Burbidge, ApJ 174 (1972) 253

V. L. Ginzburg, Astro. and Space Phys., Vol. 4, p.167 (1972)

A.W. Strong, *Nucl.Part.Phys.Proc.* 297-299 (2018) 165-170

Back in the 1970s, there was a debate about whether **all** CRs could be extragalactic. Subsequent diffuse gamma-ray observations, however, constrained such a scenario.

Isotropic Gamma-Ray Background

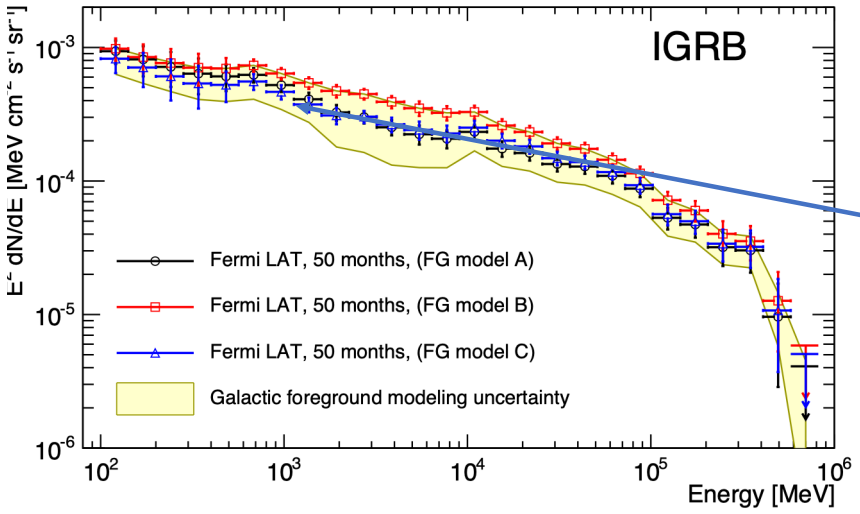

1 GeV Flux Expected for Model:

$$\mathbf{E_\gamma^2 \frac{dN}{dE_\gamma} \approx 2 \times 10^{-3}\ MeV cm^{-2} s^{-1} sr^{-1}}$$

1 GeV Diffuse Flux:

$$\mathbf{\approx 6 \times 10^{-4}\ MeV cm^{-2} s^{-1} sr^{-1}}$$

Ackermann et al., *Astrophys.J.* 799 (2015)

Features in the CR Spectrum

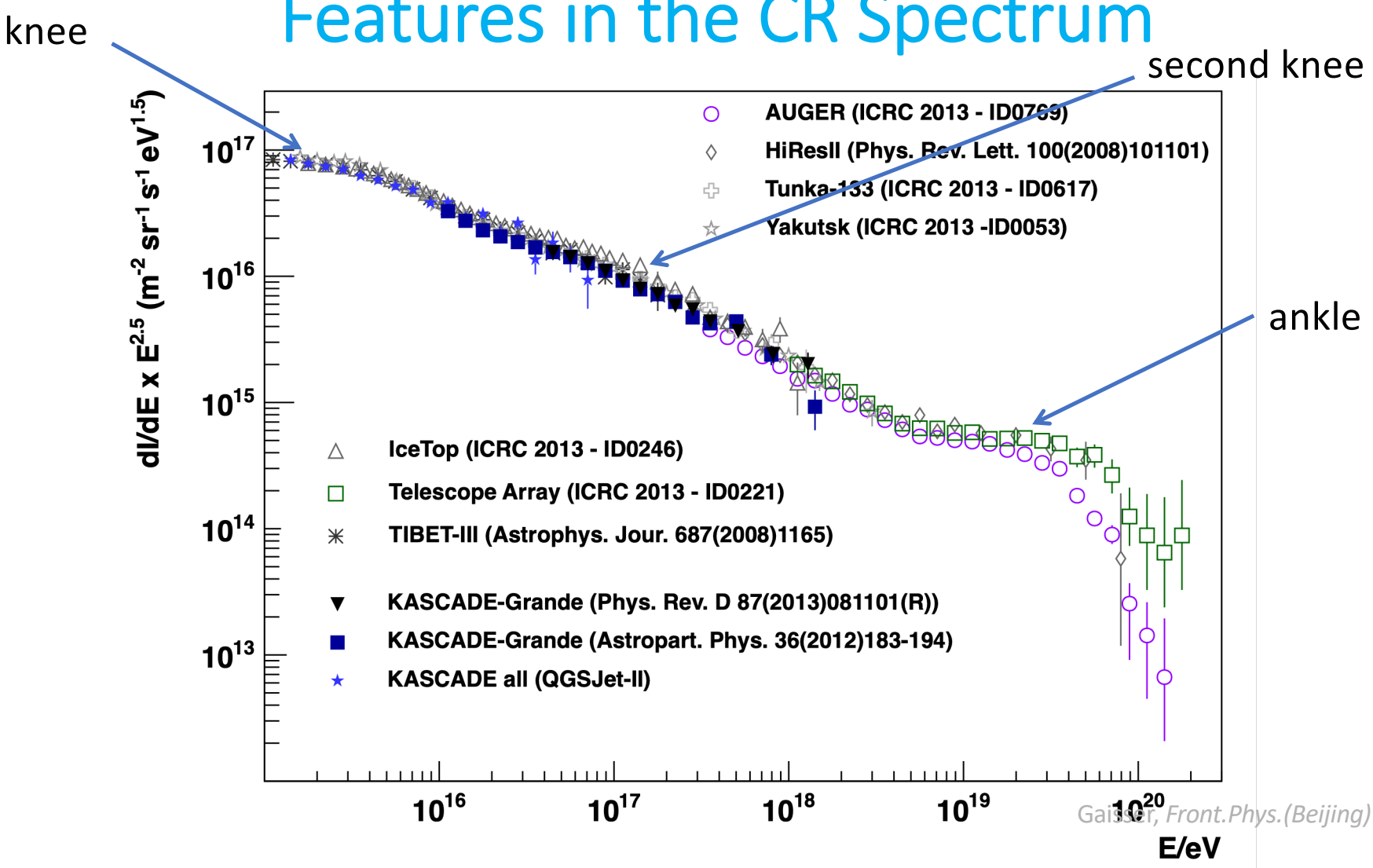

Gaisser, *Front.Phys.(Beijing)* 8 (2013) 748-758

Population B…But Whose Population B?

Constraints on at What Energy the Onset of Population B can Occur

CR Composition Evolution

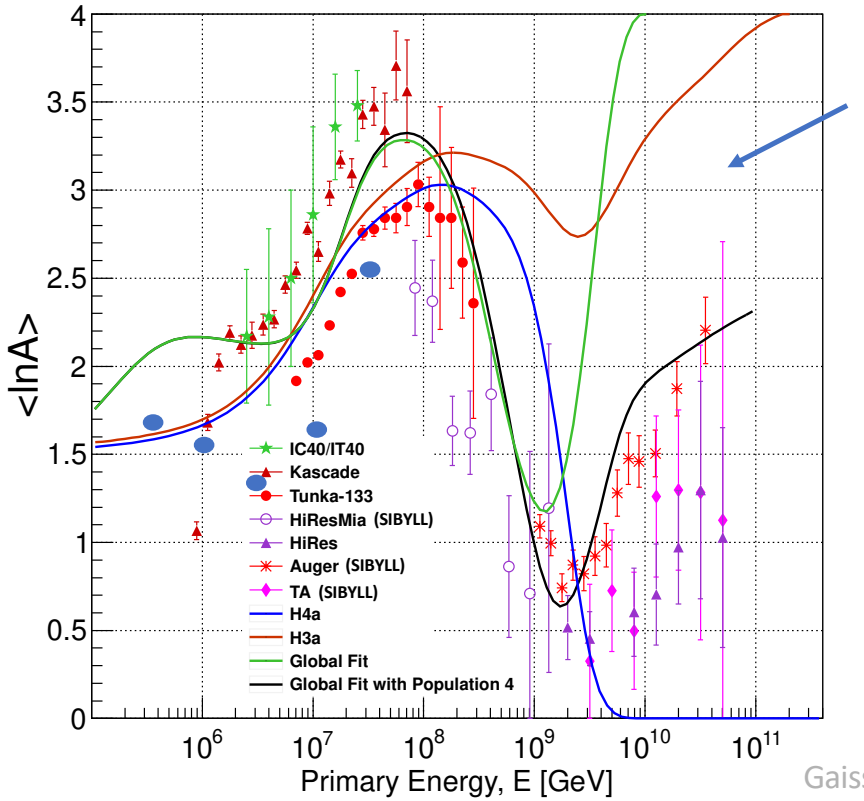

Only two clear light-heavy-light-heavy “cycles” in composition observed in data between the knee and the highest energies.

This places a strong constraint on the spacing of the energy onset in dominance of the new spectral components

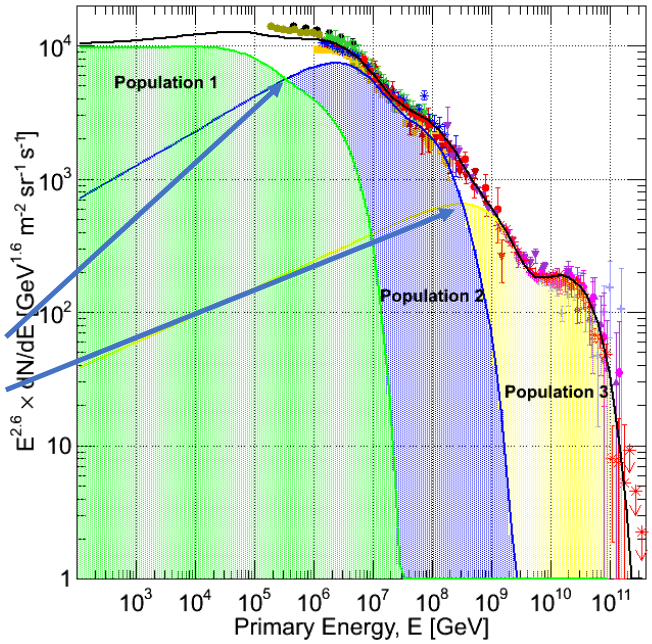

Gaisser, Front. Phys., 2013, 8(6): 748–758 (2013)

Kampert et al. **Astropart. Phys.** 35 10 660-678 (2012)